TECHNISCHE UNIVERSITÄT WIEN
Vienna University of Technology

DIPLOMARBEIT

Development of a colorimetric protein array for the detection of sepsis

Ausgeführt am Institut für Chemische Technologien und Analytik
der Technischen Universität Wien

Unter Anleitung von

Univ. Doz. DI Dr. techn. Georg Haberhauer, MBA

und

Mag. Dr. rer. nat. Claudia Preininger
AIT Austrian Institute of Technology GmbH, Department Health & Environment

durch

Heidelinde Herzog, BSc
Mitisgasse 5/2/3, 1140 Wien

Wien, am

1 Kurzfassung

In dieser Arbeit wird ein Multiplex-Immunoassay für die einfache und kostengünstige Quantifizierung von C-reaktivem Protein (CRP), Interleukin-8 (IL-8) und S-100 präsentiert, welcher auf kolorimetrischer Detektion und Auslesung mit Digitalkamera basiert.

Glas modifiziert mit Epoxy-Polymer (SU-8), Nitrozellulose und Polyvinylidenfluorid (PVDF) wurden mit Fänger Antikörpern für IL-8 und S-100, sowie mit dem Antigen CRP bespottet. Die Detektion und Quantifizierung der Biomarker im Serum wurde durch Immunreaktionen mit biotinylierten Detektionsantikörpern und Streptavidin, gebunden an entweder Gold Nanopartikel, Alkaliner Phosphatase oder Meerrettichperoxidase, durchgeführt. Die gebundenen Goldnanopartikel wurden durch Silberfärbung sichtbar gemacht. Das Auslesen erfolgte mit Clondiag ArrayMate oder einer Digitalkamera.

Die Ergebnisse zeigen, dass das zu bevorzugende Chipmaterial sehr stark von der gewünschten Detektionsart abhängt: nicht transparente Chipoberflächen zeigen höheren Kontrast und sind daher für die kolorimetrische Detektion besser geeignet als transparente Materialien. Die Sensitivität der kolorimetrischen Methode (Detektionslimits: 0,01 ng/mL für S-100; 1,34 pg/mL für IL-8; 3,00 µg/mL für CRP) war ähnlich der des auf Fluoreszenz basierenden Chip, was darauf hindeutet, dass die kolorimetrische Detektionsmethode die konventionelle fluoreszenzbasierte Methode ohne Einbußen in der Sensitivität ersetzen kann, dabei aber deutlich kosteneffizienter arbeitet.

2 Abstract

We present herein a multianalyte immunoassay for simple and low-cost quantification of C-reactive protein (CRP), Interleukin-8 (IL-8) and S-100 based on colorimetric detection using a digital camera for read-out.

Glass slides coated with epoxy-polymer (SU-8), nitrocellulose and polyvinylidenefluoride (PVDF) were spotted with capture antibodies for IL-8 and S-100 and the antigen CRP. Detection and quantification of biomarkers in human serum was performed by immunoreactions with biotinylated secondary antibodies and streptavidin labeled with gold nanoparticles, alkaline phosphatase or horse radish peroxidase. The bound nanoparticles were visualized through silver staining. The read-out was fulfilled with Clondiag ArrayMate or a digital camera.

Results demonstrate that the choice of chip substrate is crucial with respect to the selected detection method: non-transparent slides show higher contrast and are therefore more suitable for colorimetric detection than transparent slides. Assay sensitivity of the colorimetric assay (limits of detection: 0.01 ng/mL for S-100, 1.34 pg/mL for IL-8, 3.00 µg/mL for CRP) was similar to that of the fluorescence-based chip, indicating that the colorimetric approach can replace the conventional approach without compromise in sensitivity but being more cost-effective.

3 Acknowledgements

First of all I like to thank Dr. Claudia Preininger for the possibility to write my diploma thesis in her group on this exciting topic and the possibility to present my work at the Europtrode in Barcelona. I am also very grateful for the support of Patricia Buchegger during my work. Further, I would like to thank Prof. Georg Haberhauer for his advice.

Financial support of this work was provided by the project “Changes” funded by the Austrian Federal Ministry for Transport, Innovation and Technology. This project also allowed me to participate in various seminars, meet a lot of fascinating people and to be mentored by Prof. Wolfgang Knoll who gave me interesting insights and shared his experiences. I also would like to mention Gabriele Heeger-Tinhof whose charismatic coachings helped me to gain new perspectives to various matters of life, relationships and success.

I also like to thank my colleagues Jennifer, Alma, Shima, Thomas, Ursula and Geraldine for discussions, stories and laughter; not to forget the collective complaints about the lunch in the canteen. Further I would like to thank Theresa for a lot of shared hours of studying, for giving me lifts to Tulln and back, for her help and support in general and also, for her wonderful muffins.

Of course I am very thankful to my parents and my sister who supported me during my studies and also helped me to cope with difficulties. Last but not least I would like to thank all my friends for believing in me, for cheering me up and for sharing their experiences.

“The great aim of education is not knowledge but action.” (Herbert Spencer)

4 Table of contents

5 Aim

Compared with the traditional single-analyte immunoassays, parallel multianalyte immunoassays can provide higher sample throughput, shorter assay time, less sample consumption, lower cost per assay and more efficient diagnosis of the disease [1]. Protein microarray technology allows detection and quantification of a multiple set of biomarkers with small sample volumes, low reagent consumption and high sensitivity [2].

In most microarray architectures fluorescent based detection is used [3]. Fluorescence occurs when photons are absorbed by molecules and light is emitted. To induce and detect fluorescence, an excitation part (in many cases a laser beam to reach higher sensitivities) and an emission part, often combined with photomultiplier tubes, is required. Systems like these are costly and ranging from 25.000 to 220.000 USD [4]. Therefore their use and also the use of microarrays in diagnostics is limited.

In order to significantly reduce costs and provide a portable and flexible microarray system, colorimetric detection in combination with a digital camera represents a valuable alternative. However, this approach is often associated with loss in assay sensitivity and reproducibility of results.

In this work, we therefore evaluate two colorimetric detection principles (enzymatic reaction and gold nanoparticles combined with silver staining) for the simultaneous detection of S-100, IL-8 and CRP and compare the two approaches to conventional fluorescence-based chips with respect to sensitivity, reproducibility and required assay time. Basis of this method is the already established protein microarray for sepsis [5].

6 Introduction

6.1 Biomarkers

The term biomarker has been in use since at least the 1970s, initially in clinical research on cancer and cardiovascular disease [6]. A biomarker ideally varies continuously with the level of activity or degree of progression of a disease process [6]. The biomarkers definitions working group therefore defined a biomarker as "a characteristic that is objectively measured and evaluated as an indicator of normal biological processes, pathogenic processes, or pharmacologic responses to a therapeutic intervention" [7].

Biomarkers are quantitative indicators for diseases and have multiple applications:

- **Prediction**: predict patients at risk of disease
- **Detection:** identification of patients with disease
- **Staging:** classification of the extent of disease
- **Grading**: indicator of disease aggressiveness and prognosis
- **Assessment of response to treatment:** evaluating the disease response to treatment [8].

Neonatal sepsis within seven days of birth is associated with mortality rates between 15 and 50 %; the successful treatment of neonatal sepsis depends on early diagnosis as late treatments increase the possibility of long term sequelae and disability [9]. Several serum proteins, such as IL-6, IL-8, IL-10, TNF alpha, S-100, PCT, E-selectin, CRP are identified as biomarkers for neonatal sepis [10].

IL-8 is an inflammation mediator that's dominating active form consists of 72 amino acids and is mostly found as dimer; generally it can be expected upon infection, ischemia, trauma and other disturbances of tissue homeostatsis [11]. IL-8 is an important biomarker for classification of the severity of sepsis [12], the cut-off value lies at 20 pg/mL in serum [13], the cut-off values for severe sepsis and septic shock are at 87 pg/mL and 693 pg/mL respectively [14].

CRP is an acute phase protein that can rise from 50 % up to 1000-fold in pathologic response; it is build up of five identical subunits, each subunit consists of 206 amino acids with a molecular weight of approximately 23 kDa and is present in a median serum concentration of 0.8 µg/mL under physiological circumstances [15]. In infections, CRP is expressed as part of the immediate immune response, the cut-off value lies at 10 µg/mL serum [16].

S-100 proteins are involved in calcium-, zinc or copper-dependent cellular functions, they modulate the cell metabolism, proliferation and maturation by structural participation in membranes [17]. The levels of S-100 are significantly elevated in neuronal inflammations, the cut-off value lies at 10.4 ng/mL in serum [18].

6.2 Colorimetric Microarrays

Biochips are miniaturized analytical tools that are used for the detection of thousands of molecules at the same time. On the chip surface a probe is immobilized which binds specifically to the target molecule and therefore allows proof of a certain compound. It is important that the position of every probe is exactly defined. In nearly all biochip systems the probes are applied in an x-y-grid with an exact definition which probe is applied at which location. Because of the geometric assembly, biochips are also called microarrays (micro: small, array: assembly in a grid) [19]. The necessity to distinguish the specific response of each different spot has led to an intensive utilization of fluorescence imagers and scanners. Despite the fact that fluorescent detection is giving very good results when high sensitivity and resolution is required, high costs have negative impact on wide distribution of the tool [20]. However, reports on successfully using more cost-effective colorimetric approaches in microarray technology are still limited.

In literature, colorimetric detection was implemented in both DNA and protein arrays. For example, 2004 Liang et al. reported the application of a gold-silver detection method in analyzing protein microarrays. IgG was spotted onto modified glass slides to detect anti-IgG in solution, the results indicated that the gold-silver colorimetric method using a CCD camera for read-out is able to reach limits of detection of 2.75 ng/mL, which is close to the sensitivity of the fluorescent detection method [21]. Jiang et al. (2008) developed a colorimetric detection based protein microarray for serodiagnosis of ToRCH infections. Arrays with an agarose modified surface provided a three-dimensional structure for the immobilization of TORCH antigens. The arrays were processed with human serum and colloidal gold-labeled goat anti-human IgM antibodies and made visible by silver staining; read-out was fulfilled with a flatbed scanner. The results of the immunogold-based assay corresponded well to the results of fluorescence based detection and to the results of ELISA tests [22]. Tang et al. (2009) developed a colorimetric DNA microarray for the detection of *HIV-1* and *HCV*. Oligonucleotides were spotted on glass slides and incubated with biotinylated PCR products. Through binding of streptavidin-gold and processing in silver staining solution, amounts of target DNA amplicons down to 10^2 copies/mL could be observed with naked eye [23].
Petersen et al. (2006) reported a DNA microarray for the detection of mutations in the ß-globin gene which uses colorimetric staining and visualization with a flatbed scanner. Among the different slide types used, only agarose slides and slides with nitrocellulose coating showed detectable results for the alkaline phosphatase reactions. Though the colorimetric staining of arrays was performed with similar or better sensitivity than the

fluorescent detection method, the dynamic range was reduced by approximately 10-fold compared to fluorescence [24]. Cretich et al. (2010) developed a colorimetric DNA microarray for easy identification of foodborne pathogens. A nitrocellulose film was used to covalently bind short oligonucleotide fragments, oligonucleotide concentrations ranging from 0.05 to 1.5 µM were clearly visible when detected with alkaline phosphatase and BCIP/NBT as substrate [25]. Wei et al. (2011) reported a glass immunoassay chip for the colorimetric detection of tumor markers using alkaline phosphatase and horseradish peroxidase for detection. The preparation of the immunoassay chip and their detection schemes were simple and inexpensive and reached detection limits of 0.25 ng/mL for the carcinoembryonic antigen CEA and 1.25 U/mL for the carbohydrate antigen CA19-9 [1]. Le Goff et al. (2012) tested different surfaces for their performance in colorimetric detection with alkaline phosphatase, BCIP/NBT as substrate and a flatbed scanner for read-out. Important for successful colorimetric detection was the capacity of the chip substrates to retain precipitating colored product, therefore, porous surfaces and adhesive surfaces led to highest signal intensities [20].

6.3 Protein Microarray Technology

A protein microarray allows the identification and quantification of a high number of proteins within one experiment [26]. The miniaturization leads to higher sensitivities, which can be explained by the ambient assay theory [27] shown in Figure 1.

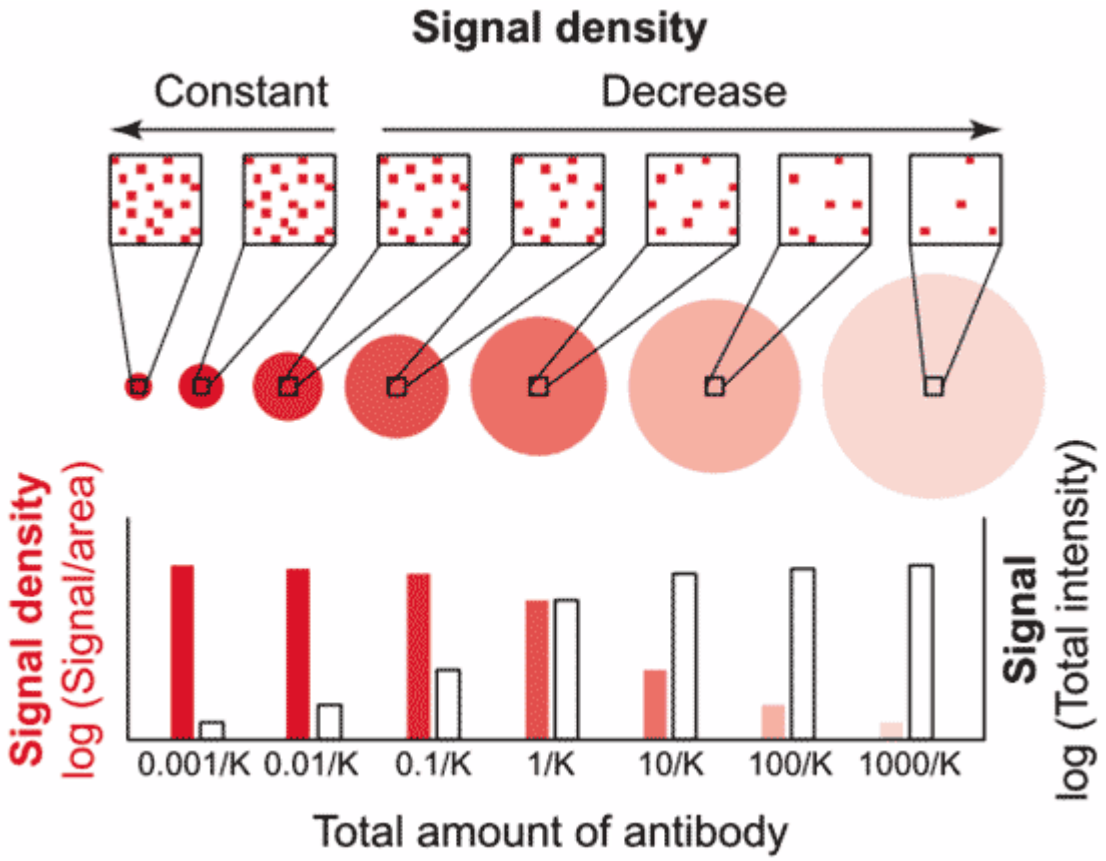

Figure 1: Ambient assay theory according to [27]. When spot diameters are enlarged, larger amounts of capture molecules (here: antibodies) are bound to the surface. The total signal intensity (signal intensity of the whole spot) therefore also rises until the maximum is reached (all molecules in the sample are bound to the spot). Therefore, the measurement is not representative if the sample contains a small amount of target molecule; also the maximum signal intensity per area is limited. When the target molecule is bound to spots with small spot diameter the signal density rises and reaches a constant value when the antibody concentrations is smaller than 0.1/K (K=affinity constant). The complexes between capture and target molecule are built in very small areas which lead locally to high signal intensities.

The development of protein arrays lagged behind of DNA arrays because of the greater complexity of proteins. DNA molecules are homogenous molecules with very similar chemical and physical properties whereas proteins consist of more building blocks and therefore are diversely charged, have different solubilities and partly show less stability [26]. Also, protein microarrays must be able to detect low-abundance proteins without an amplifying technology like PCR (polymerase chain reaction). Chip surfaces must immobilize capture agents without causing conformational changes [4].

Multiplexed immunoassays are the most developed application of protein arrays, one of the most used strategies is the miniaturization and multiplexing of the standard enzyme linked immunosorbent assay (ELISA) [28]. Compared with the traditional single-analyte immunoassay, multianalyte immunoassays can provide higher sample throughput, shorter assay time, less sample consumption, lower cost per assay and more efficient diagnosis of the disease [1].

6.3.1 Substrates

The choice of chip substrate depends on the production procedure, the application and the detection method. In Figure 2 various types of substrate are presented.

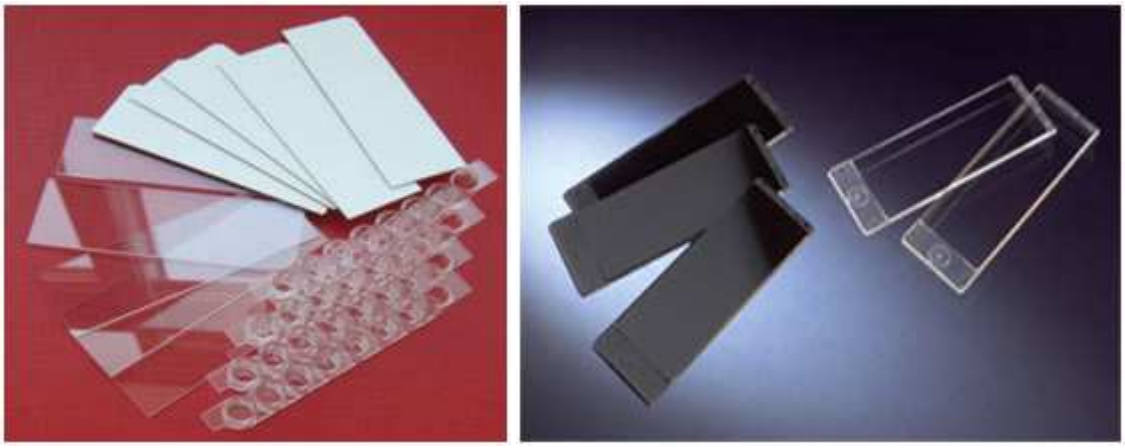

Figure 2: Different chip substrates: left: Glass Chips, modified with an epoxy coating (ARChip Epoxy, transparent) or with a nitrocellulose membrane (SuperNitro of Arrayit, white) and Plastic Tubes (Scienion strips). Right: Microarray Slides MaxiSorb™ made of dark or clear polymer from Nunc (www.nuncbrand.com)

Glass is a very popular chip substrate due to its chemical resistance, thermal stability and low intrinsic fluorescence. It also allows incident and transmitted light for the detection and can be purchased with various chemical surface modifications. Glass attached with three dimensional structures such as agarose or membranes are very suitable for colorimetric detection methods. If detection via surface plasmon resonance is required, glass slides can also be modified with metal surfaces. Slides with mirrored surfaces promise higher sensitivities.

Polymers, such as polystyrene, polycarbonate and ZEONOR allow various architectures with limited intrinsic fluorescence. So-called array tubes which are plastic strips that can be used with common laboratory equipment such as heating blocks and centrifuges allow easy handling. However, polymers are still not commonly used due to their poorer optic and mechanical properties compared to glass.

6.3.2 Protein Immobilization on Surfaces

The extreme diversity and complexity of proteins make predictions regarding attachment to the surface difficult. In contrast to DNA, proteins have many different structures, contain heterogeneous hydrophobic and charged domains, are extremely fragile with activity dependent on retention of three-dimensional structure and can have multiple interaction sites. Functional conservation and sufficient concentration of bound protein are critical to the success of the technology [28]. Coupling of a protein to a surface is often fulfilled with compromises [3]. Protein binding to surfaces can be achieved based on five binding principles: covalent, electrostatic, site-specific affinity binding, three-dimensional and adsorption.

6.3.2.1 Covalent binding

The biochip surface is modified with e.g. aldehyde or epoxy groups to make covalent binding of macromolecules possible. The reactive groups are schematically shown in Figure 3. While aldehyde binds to the hydyroxyl groups of glass and to proteins under formation of a Schiff base, epoxy surfaces provide very reactive electrophylic groups which bind to amines under ring-opening and formation of a secondary amine [3]. ARChip Epoxy is manufactured by coating precleaned glass slides with SU-8 inmethylethylketone [29].

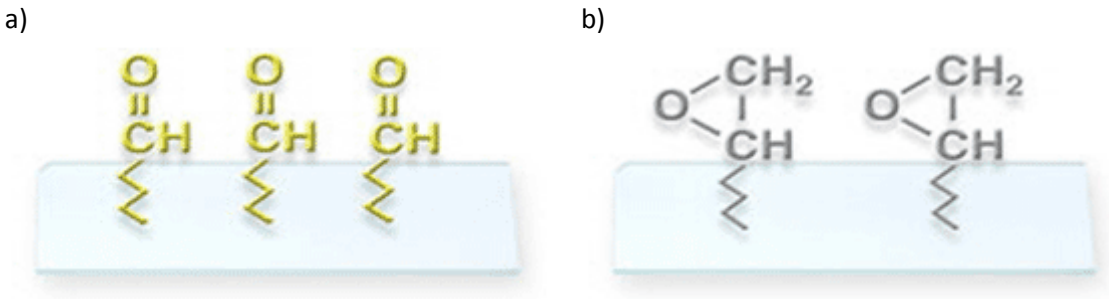

Figure 3: Slides with left: aldehyde and right: epoxy modification (www.arrayit.com)

6.3.2.2 Electrostatic binding

Biochips coated with 3-Aminopropyltrimethoxysilane (“Aptes”) or Poly-L-lysine are widely used as substrates for electrostatic binding. Thereby negatively charged groups of the protein interact with the positively charged amino group of the chip surface. However, aminosilane surfaces are more suitable for immobilization of DNA than proteins, as DNA (in contrast to proteins) is homogeneously negatively charged. The exact orientation of the binding molecules is not predictable [3].

6.3.2.3 Affinity binding

In affinity binding, the surface is modified with a certain molecule and the probe is modified by the binding partner of the molecule, such as biotin and streptavidin, Ni^{2+} chelates and histidine or DNA directed binding. In the avidin-biotin system the chip surface is modified with avidin, DNA or proteins are biotinylated which results in site-specific binding of the probe. Surfaces can also be coated with Ni^{2+}or Cu^{2+} chelates, the probe is then modified with a so-called (poly) his-tag which consists of 5 to 10 histidines and binds to metal matrizes. In DNA directed binding, the surface and the probe is modified with complementary DNA sequences which bind by hybridization.

6.3.2.4 Three dimensional binding techniques

When three dimensional techniques are used, the probes are not only bound to the surface but also immobilized in a matrix which allows immobilization of high amounts of probes. Therefore, layers of polyacrylamide or agarose gels and also membranes, such as nitrocellulose or polyvinylidene fluoride (PVDF) are used [19]. Nitrocellulose binds proteins through hydrophobic interaction and is easily wetted, the good binding capacity and low background make nitrocellulose to the most popular membrane in analytical protein chemistry [30]. The surface topography of nitrocellulose is shown in Figure 4. As a result of the porous character slides with nitrocellulose coating show bigger spots [20]. Hydrophobic PVDF membranes are mechanically and chemically stable but show lower protein binding abilities than nitrocellulose [31].

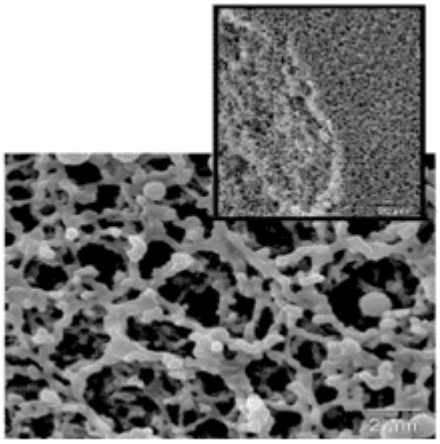

Figure 4: Scanning electron image of Nitrocellulose at 2 µm and 20 µm scale respectively. [20]

6.3.2.5 Adsorption

Large molecules, like antibodies (150 kDa) have the ability to adsorb on surfaces; the orientation in this case is random.

6.3.3 Probe arraying

Probe arraying or spotting is the process that brings the biomolecules onto the chip substrate. So-called arrayers or spotters print biomolecules precisely on different positions and in small volumes. High precision is needed as very small volumes (few nanoliters) are applied on a defined point in an x-y-grid. The size of the spot is usually between 100 and 200 µm, the application of such small volumes (nL to pL) is possible through capillary forces [19]. It is of great importance for the arraying process that all components are ultrapure or at least filtrated with a pore diameter of 0.22 µm². The viscosity of the buffer needs to be high enough to reach the desired spot diameter [3].

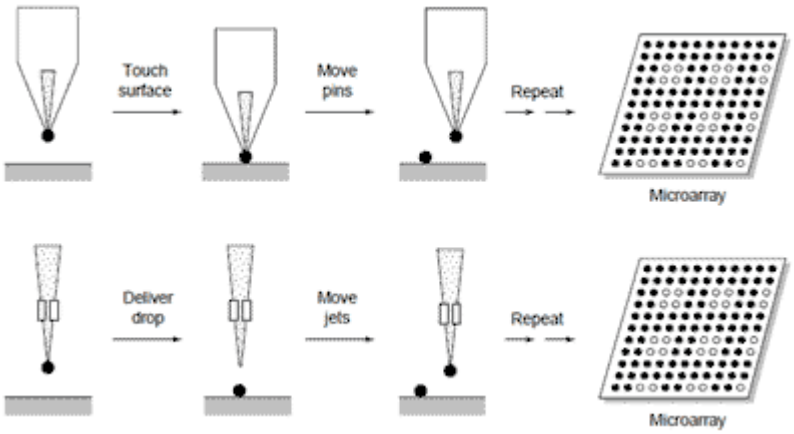

Figure 5: Schemes of contact and non contact printing [32].

Contact printing is accomplished by loading the sample into a spotting pin by capillary action and transfer to the surface upon physical contact. The spotting principle is described in Figure 5. Advantages are the rapid implementation, low cost and versatility [32]. Pins usually consist of steel or titan, “solid pins” have to be washed and dried after the print of every spot, while “splitted pins” allow printing of several spots as liquid is trapped in the pin through capillary forces. Ring-and-Pin-Systems contain a reservoir and therefore, also allow printing of several spots in one run [3].

Non contact printing or ink jetting is fulfilled without physical contact to the surface by piezoelectricity and is similar to the functionality of customary inkjet printers. A flexible tube is surrounded by ceramic, if an electric impulse is applied on the ceramic, the tube constricts and releases the probe without the necessity of the pin to touch the surface [3].

First introduced by Kumar and coworkers in 1993, micro contact printing (µCP) became an accepted method for printing materials on solid surfaces.

In a µCP process, an elastomeric stamp made of polydimethylsiloxane (PDMS) is molded against a siliconmaster with micropatterns on its surface to create microstructures [33]. The stamp is then "inked" with a solution of the compound to be patterned, dried by evaporating the solvent and then brought into contact with the substrate and the chemistry, therefore, is transferred only in those regions where the stamp relief comes into the direct physical contact with the surface [34] (see Figure 6 for details).

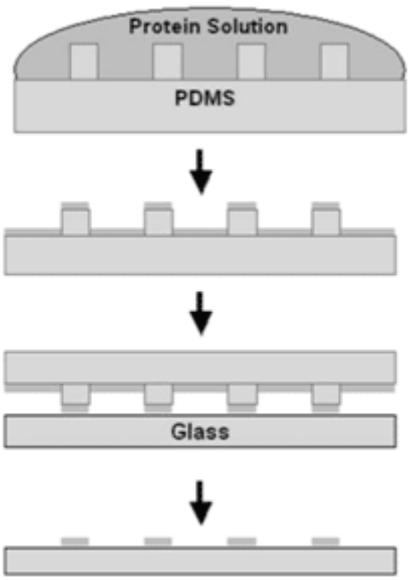

Figure 6: Scheme of micro contact printing from [34].

6.4 Microarray processing

Protein microarrays can deliver qualitative and quantitive information. Protein microarrays can be used for all interactions where molecules bind each other specifically, such as protein-protein interactions, antigen-antibody reactions, enzyme-substrate and ligand-receptor interactions [26]. Arrays can also be produced from cell or tissue lysates or even whole cells.

6.4.1 Reverse phase assays

In a reverse phase assay, the analyte of interest is immobilized on the slide to be detected by the recognition element which is present in solution. Whole protein-fractions of cells or tissue sections are immobilized on the surface. Through addition of antibodies, the whole proteome of this cells or tissue sections can be examined for the existence of certain antigens [26]. Detection can be done with a directly labeled antibody or through reaction with a labeled secondary antibody as shown in Figure 7. This method is only limited by the availability of specific antibodies for the antigens examined.

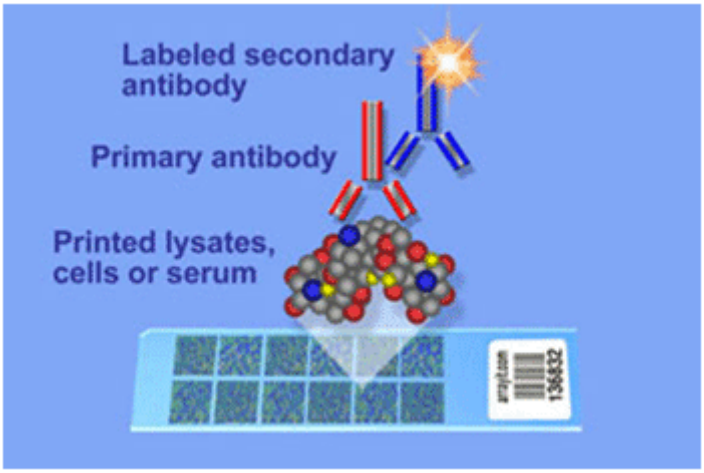

Figure 7: Reverse phase assay detected with a labeled secondary antibody (www.arrayit.com)

6.4.2 Forward phase assays

In a forward phase assay, the recognition element is spotted on the slide to capture the analyte of interest in solution. Such protein arrays are mainly used for the analysis of antigen-antibody interactions. Thus, a high number of either antibodies or antigens is immobilized on a surface to then bind the corresponding antibody/antigen in the liquid sample [26].

Protein-protein interactions can be observed as shown in Figure 8. Proteins or protein domains are immobilized on a chip surface, the chip is then incubated with the sample.

The sample can be labeled or the array can be detected with a label-free technique. A commercially available example is an array of Invitrogen which contains more than 4000 immobilized proteins of *Saccharomyces cerevisiae* and control proteins that enable screening of nearly the whole yeast proteome for interaction partners [26].

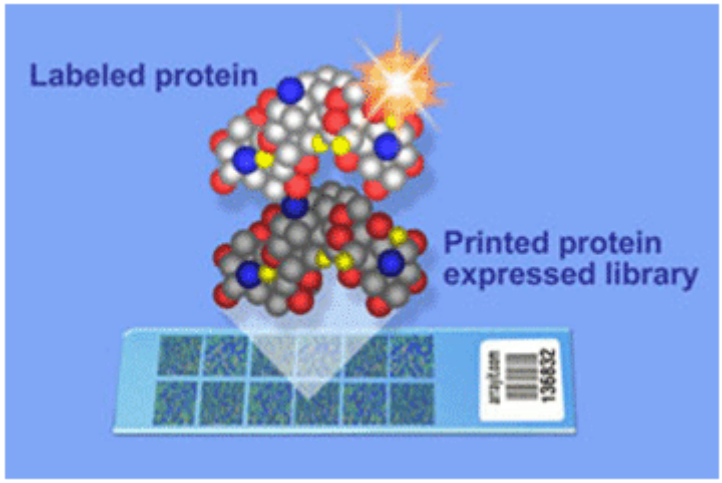

Figure 8: Array for the examination of protein-protein interactions (www.arrayit.com)

6.4.2.1 Sandwich assay

For the sensitive detection of an analyte, miniaturized sandwich arrays are commonly used. Similar to the principle of ELISA (enzyme linked immunosorbent assay), a capture antibody is immobilized on the surface [26]. The analyte in liquid phase is then bound by this antibody; a so-called detection antibody binds to another epitope of the antigen creating a “sandwich”. The detection antibody carries a label that generates a signal; the signal intensity correlates to the amount of bound biomarker. Figure 9 shows a scheme of this assay. Through the use of two antibodies high selectivity is granted. This method allows implementing miniaturized, multiplexed ELISAs in parallel.

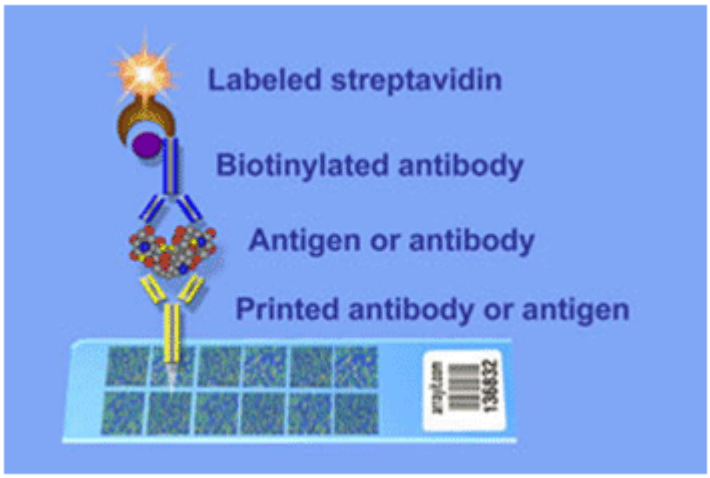

Figure 9: Scheme of a sandwich microarray (www.arrayit.com)

6.4.2.2 Competitive assay

The competitive assay is suitable for analytes that are too small to bind two antibodies. The capture antibody is immobilized on the chip substrate; meanwhile, labeled analyte is mixed with the sample. The analyte of the sample and the labeled analyte are competing for binding sites on the chip surface. The signal intensity decreases with higher concentrations of antigens in the sample.

6.4.2.3 Binding inhibition assay

In the binding inhibition assay, the antigen is immobilized on the surface. Meanwhile, labeled detection antibody is added to the sample which binds to the antigens present. When the sample mixture is applied onto the biochip, only detection antibodies that did not bind an antigen in the sample can bind to the immobilized antigen. Therefore, the signal intensity decreases with higher concentrations of antigens in the sample.

6.4.2.4 Comparative assay

Two complex protein samples, one for referencing and an experiment sample are labeled with different fluorochromes. The samples are then mixed and incubated with an antibody array. The ratio of the two dyes found in one spot corresponds to the relative concentration of each protein in the two samples [35]. It is also possible to array antigens and detect antibodies which can be suitable for the detection of autoimmune diseases [28].

6.4.3 Other

Other assay formats are used to examine enzyme-substrate interactions or ligand-receptor interactions; even whole cells or tissues can be arrayed on a chip [26].

6.5 Optical Detection

Protein detection systems are divided into label-based and label-free technologies. Label-based systems require modification with a label; this can be conventional fluorescent dyes, such as fluorescent particles, quantum dots, enzymes and gold nanoparticles. Label-based methods widely used are fluorescence, absorption and chemiluminescence. Label-free detection techniques include surface plasmon resonance (SPR) and reflectometric interference spectroscopy (RifS).The majority of microarray applications use label-based detection techniques [36].

6.5.1 Fluorescence

Basis of Fluorescence is the absorption of photons which excite the system electronically and vibrationally. When the system relaxes, light is emitted. The emitted photons have longer wavelength and lower energy than the absorbed radiation. The shift of the fluorescence spectrum to lower energy (Stokes shift) can be enhanced by solvent interactions. The quantum yield [Φ] is the ratio of emitted photons to absorbed photons and can be calculated by the rate constants for fluorescence [k_f] and deactivation [$k_{deactivation}$]:

$$\Phi = \frac{k_f}{k_f + \sum k_{deactivation}}$$

According to Lambert-Beer law, the intensity of the fluorescent signal depends on the concentration, the quantum yield and the extinction coefficient of the fluorophore [37].

The optical setup of fluorescent detection involves an excitation part and an emission part. The emission of light will continue until the excitation source is turned off or the fluorophore is photodecomposed. Common excitation sources include laser, light-emitting diodes (LED) and mercury or xenon arc lamp. Figure 10 shows one of most commonly used excitation system in microarrays which is laser-induced fluorescence (LIF) [38]. The complexity of a microarray scanner increases with the number of fluorophore dyes because each dye requires a different excitation wavelength. Microarray scanners must show high resolution as spots in µm distance must be differed significantly. As explained in Figure 10 a laser beam goes through an excitation filter, a laser splitter and an optical lens and reaches after that bundled and focused the microarray. Fluorophores absorb the laser light and emit light of a higher wavelength that goes through an optical lens, a laser splitter, a mirror, an emission

filter and to the photo multiplier tube (PMT) [3]. As the PMT is a point detector, it requires sophisticated scanning stages [39].

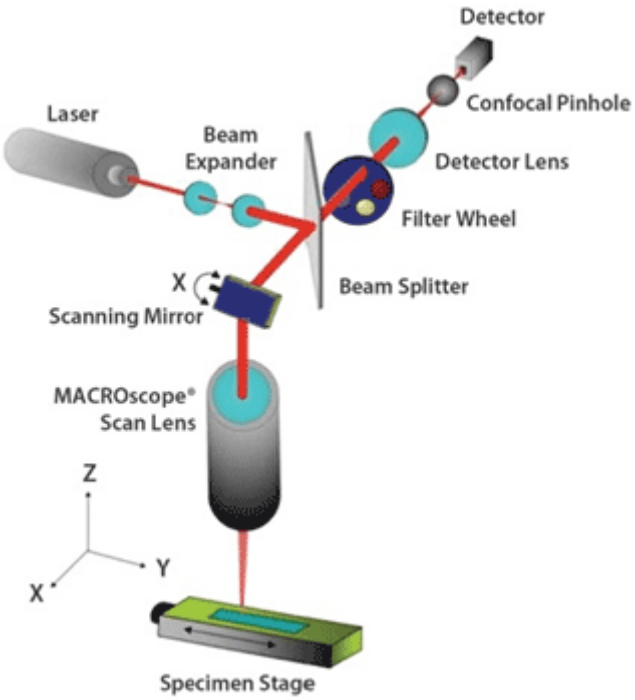

Figure 10: DNAScope™ laser confocal scanner (www.biocompare.com)

Another possibility is to use white, polychromatic light for excitation which travels through filters and lenses and then to a camera [3]. The camera makes pictures of bigger areas of the microarray and stitches them to a picture of the whole array [3]. A CCD (charge coupled device) is a photo sensor that uses an array of silicon diodes that transforms the emitted photons into electric charge [3].

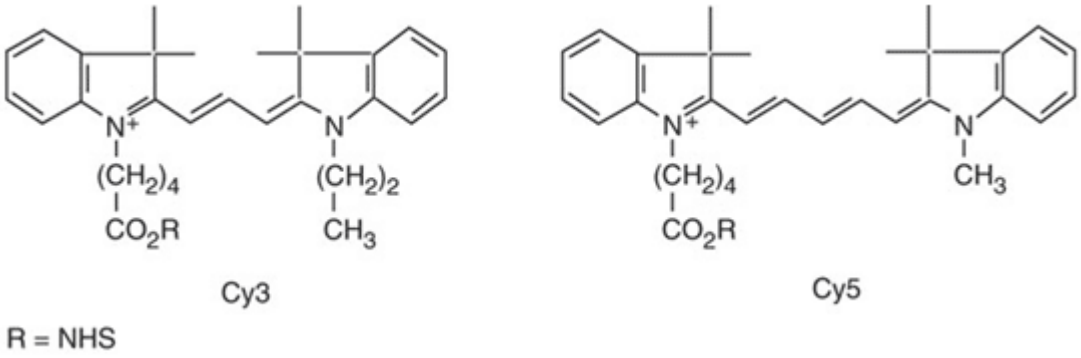

Figure 11: Cyanine-3 and Cyanin-5 modified (www.nature.com): The fluorescence is dictated by the carbon polyene chains which are linking the two indoline rings.

The fluorophore labels most commonly used in microarrays are Cyanine 3 (Cy3 – green; excitation: 530 nm, emission: 550 nm) and Cyanine 5 (Cy5 – red; excitation: 650, emission: 670) as they are associated with good signal strength and limited dye

interactions. Alexa dyes are highly substituted fluorescein derivates that exhibit higher brightness, more photo stability and less quenching than cyanine dyes [39]. Alexa Dy647 with the molecular formula $C_{32}H_{37}N_2O_8S_2$ is a red fluorescent dye (excitation: 636 nm, emission: 657 nm in ethanol) that shows spectral similarity to Cy5 and can be purchased with various modifications such as streptavidin for the use in a biotin-avidin system [40].

The appropriate choice of fluorophore molecules relies on the substrate used, the light emission spectra of the dye and the number of target proteins in the sample. Typically, target proteins are captured by antibodies immobilized on the array surface, and detected using a secondary antibody attached to a fluorophore or even an additional streptavidin-biotin system which offers higher specificity [36].

6.5.2 Colorimetry

The major advantage of colorimetric labels is the option of visual detection, which makes it possible to develop simple, cost-effective and user-friendly assays [41]. A chromophore is the part of a molecule that contains excitable electrons and is responsible for the color of the molecule as their interactions take place in the visible spectrum. Chromophores are often conjugated π-electron systems; after absorption of light of a certain wavelength the remaining light is reflected by the surface or passes through transparent materials and is perceivable as color [42]. Typical colorimetric detection systems used in biochemistry are enzymatic detection and gold label silver staining as indicated Figure 12. Colorimetric detection can be accomplished with less complexity in technical equipment. An objective and a light sensitive layer are sufficient for the detection; such a system may be our eyes or customary devices like cameras or scanners. In Figure 13 a commercially available colorimetric system, consisting of a flatbed scanner and microarray software, is shown.

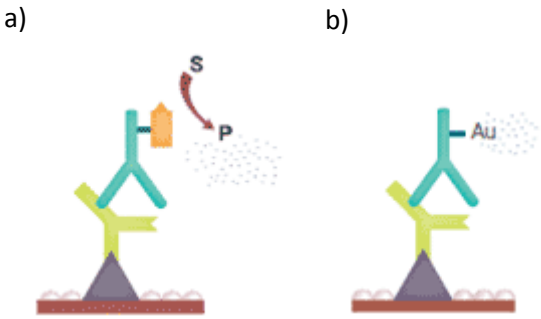

Figure 12: Modified from www.biorad.com. Colorimetric detection principle in two different assay formats. a) Enzymatic detection: a chromogenic substrate is converted to a colored product b) Gold nanoparticles are bound to the secondary antibody, silver staining can be used to enhance the signal intensity.

Figure 13: Example of a colorimetric detection system (www.arrayit.com)

6.5.2.1 Enzymatic labels

The advantages of working with enzymes are their high catalytic activity, selectivity and the sensitivity obtained by strong signal amplification. Enzymes must fulfill several demands like high stability and a pH optimum that corresponds to the assay conditions at low cost [43]. In enzymatic reactions, a detectable signal is generated by the action of the enzyme on a chromogenic substrate. In microarrays with sandwich architecture the enzyme is bound by the detection antibody or streptavidin and therefore accumulates at spots where biomarker has been captured. The enzymatic reaction with chromogenic substrates leads to the precipitation of a colored product at the side of the conjugated enzyme and therefore, analyte of interest [30]. The intensity of the product and therefore, color change is proportional to the quantity of bound biomarker. Enzymes like alkaline phosphatase (“AP”) that catalyzes dephosphorylation and horseradish peroxidase (“HRP”) that catalyzes oxidation convert several substrates to a colored product; the reaction can be stopped when the desired signal intensity is reached [44].

6.5.2.1.1 Alkaline Phosphatase

According to [31] the widest spread substrates for reactions with alkaline phosphatase (“AP”) are 5-bromo-4-chloro-3-indolyl phosphate and Nitroblue Tetrazolium (BCIP/NBT) which leave a black-purple precipitate. The reaction is linear and sensitive;

the signal strength can be influenced by the incubation time [31]. Figure 14 indicates the reaction of BCIP/NBT with alkaline phosphatase: AP dephosphorylates BCIP which leads to a bromochloroindoxyl intermediate. The indoxyl is oxidized by NBT to produce an indigoid dye (purple). The NBT is reduced by the indoxyl, opening the tetrazole ring to produce insoluble diformazan (blue). The combination of the two precipitates forms a purple-blue colored insoluble product [44].

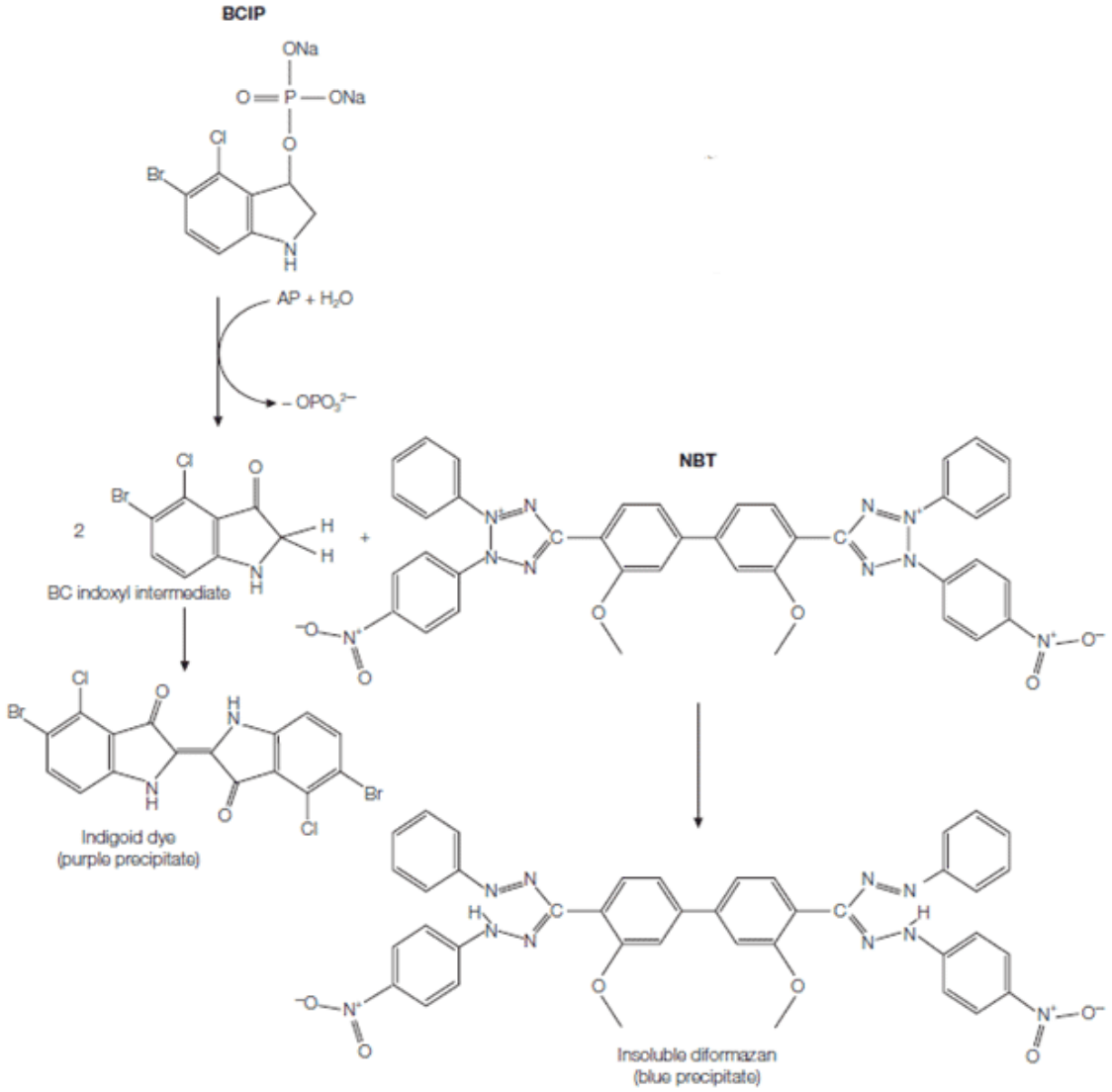

Figure 14: Reaction of BCIP/NBT with alkaline phosphatase [44].

6.5.2.1.2 Horse radish peroxidase

HRP systems are very economical as both the enzyme conjugates and the substrates can be obtained at low cost. The horse radish peroxidase system needs hydrogen peroxide as oxidizing agent. Figure 15 shows the reaction of Diaminobenzidine (dab) with hydrogen peroxide and horse radish peroxidase: in presence of H_2O_2, HRP catalyzes the oxidation of dab to a brown precipitate that is resistant to alcohol. The

sensitivity can be enhanced by addition of Ni^{2+} and Co^{2+}. The reaction can be very fast which may result in overdevelopment. Dab is a potential carcinogen and needs to be handled carefully [31]. The HRP systems are reported to be less sensitive than AP colorimetric detection systems [31].

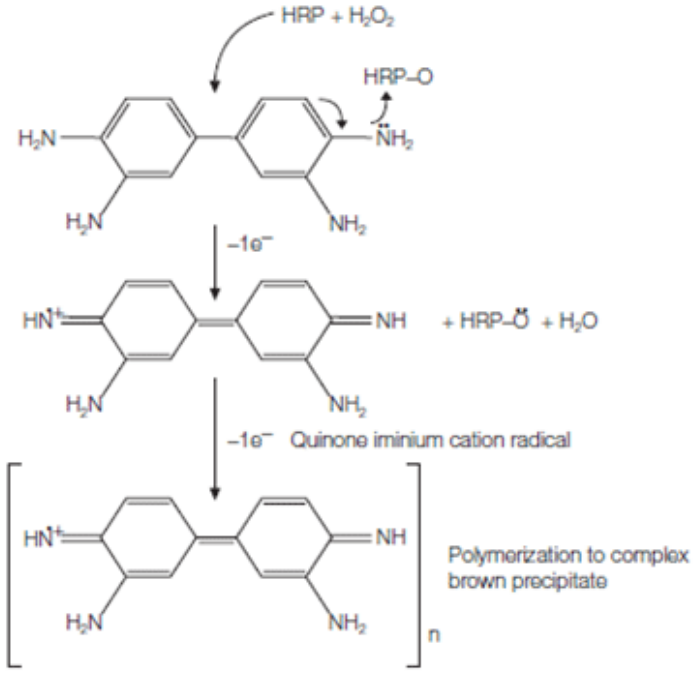

Figure 15: Reaction of dab and H_2O_2 with horse radish peroxidase [44].

Tmb is a chromogenic substrate that is commonly used in immunohistochemistry and ELISA. As can be seen in Figure 16, tmb forms the blue 3,3',5'5-tetramethylbenzidine diimine when oxidized. Tmb is photosensitive and therefore must be kept out of direct sunlight.

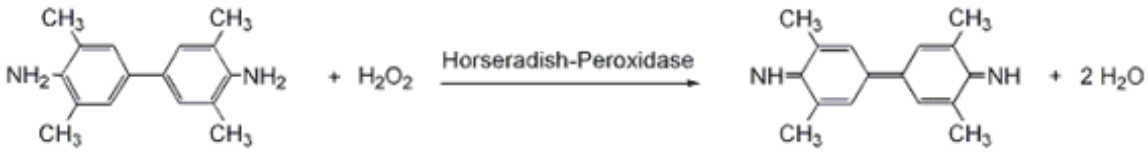

Figure 16: Reaction of tmb and H_2O_2 with horse radish peroxidase (www.biosynth.com)

6.5.2.2 Gold label silver staining

Metal nanoparticles exhibit unique optical, catalytic and electronic properties and can be used in a variety of detection schemes based on different modes of signal transduction. Gold nanoparticles (AuNP) are produced by reduction of chloroauric acid. The produced particle size influences the properties of the solution; therefore the control of particle size is of great importance in production. In transmission electron

microscopy (TEM) AuNPs are used to increase the contrast. In microarrays gold nanoparticles are typically bound to the detection antibody or streptavidin, resulting in an accumulation of gold particles to the spot were biomarker is immobilized [21].

AuNPs often need to be made visible by silver enhancement or silver staining. Silver enhancement of the gold nanoparticles produces a stable reaction product and enhances sensitivity. A scheme of the silver enhancement can be seen in Figure 17. Gold particles reduce silver ions in solution, which leads to deposition of silver on top of the gold and the growth of the metallic particle [44]. The silver shell also auto catalyzes further silver depositions. At the end of the reaction, silver deposit onto gold particles leads to an up to 100fold increase in particle size. Silver deposit strongly reflects light in the visible spectrum; the high sensitivity of this method is caused by an increase in particle volume of around 1 million times compared to the initial volume. This enhancement allows visual detection of the labeled spots and a straight-forward analysis using a colorimetric detector [45]. Silver solutions are sensitive to UV. As a consequence spontaneous conversion of silver solution into metallic grains can occur. The handling has to be as clean as possible and the silver precipitation reaction must be controlled carefully. The background increases with incubation time [45]. The quantity of the silver precipitation on each spot is proportional to the quantity of bound biomarker.

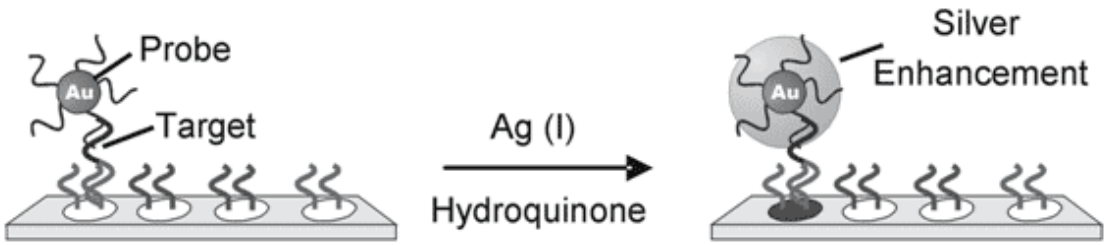

Figure 17: On a spot bound AuNPs are enlarged with silver staining [28].

7 Materials and Methods

7.1 Materials and Reagents

Proprietary ARChips Epoxy (EP 02799374; US 10/490543) and SuperNitro, SuperNylon and SuperPVDF slides obtained from Arrayit (USA), Permanox® cell culture slides from Nunc (Germany), Nexterion Aldehydsilane coated Slides and Epoxysilane coated Slides purchased from Schott (Germany) and SU8 spincoated on Zeonex (micro resist technology, Germany) were used as substrates for spotting. SD1 General Sample Diluent was from Immunochemistry Technologies (USA), Buf049A HISPEC Assay Diluent from AbD serotec (Germany). Human procalcitonin (PCT) was from Prospec (Germany). Human S-100, anti-S100 (clone 8B10), biotinylated anti-S100 (clone 6G1) and CRP-free serum for spiking experiments were ordered from Hytest (Finland). Recombinant human IL-8, anti-IL-8 (clone H8A5) and biotinylated anti-IL-8 (clone E8N1) were purchased from Biolegend (USA). CRP antigen grade, anti-CRP (clone C5) and biotinylated anti-CRP (clone C7) were from Meridian (USA). Dy647-streptavidin was from Dyomics (Germany). Alkaline phophatase-streptavidin and horse radish peroxidase-streptavidin were ordered from Biozym Biotech Trading GmbH (Austria). Horse radish peroxidase polymer-streptavidin, streptavidin-gold (40 nm) from *Streptomyces avidinii*, silver enhancer kit, Chloroauric acid ($HAuCl_4$), polyoxyethylene-sorbitanmonolaurate (Tween 20), NCIP®/BCT tablets, 3,3'-Diaminobenzidene tablets, 3,3',5'5-Tetramethylbenzidine (tmb) liquid substrate system, 3-[(3-Cholamidopropyl) dimethylammonio]-1-propanesulfonate (CHAPS) and H_3NO*HCl were purchased from Sigma (Austria). Phosphate-buffered saline (PBS) 10x (pH 7.2) was from Gibco/Invitrogen (Austria). EDC (1-Ethyl-3(3-dimethyl-aminopropyl)carbodiimid) was purchased from Fluka Biochemicals (USA).

7.2 Microarray fabrication and processing

7.2.1 Preparation of BSA conjugates

S-100/BSA conjugates were prepared as described in [10]. Briefly, 0.5 mg S-100 was incubated with 1 mg EDC for 10 minutes. Additionally, 0.5 mg BSA in 0.2 M Soren's phosphate buffer (pH 7.4) was added and the reaction was allowed to proceed for 4 h.

7.2.2 Microarray printing

0.5 mg/mL anti-IL-8, 0.5 mg/mL anti-S100 and 0.5 mg/mL CRP were spotted in triplicates onto the slides using the Omnigrid contact spotter from GeneMachines (pin SMP3). The choice of print buffer was a result of previous studies [29, 30]. As reported

by Domnanich et al. [46] print buffer “na” (1x PBS (pH 7.2)/ 0.01 % sodium-deoxycholate) was most suitable for antibody arraying.

For proteins and BSA conjugates printing buffer “cb” (1x PBS (pH 7.2) / 0.005 % CHAPS, 0.01 % BSA) was used, 0 ng/mL to 400 ng/mL S-100/BSA conjugates were spotted on the chip. The appropriate spotting conditions were reported in [46]. To prevent immediate evaporation, spotting was fulfilled at a relative humidity of 50 %. 12 identical arrays with 1-3 replicates were spotted and the spot-to-spot distance was 400 µm. After spotting, the slides were kept at 4 ° C for a minimum of 4 days to ensure capture antibody immobilization.

7.2.3 Blocking and Immunoassays

Immediately before slide processing, the slides were blocked for 30 min in 1x PBS (pH 7.2)/0.1 % Tween 20 or in 1x TBS [50 mM Tris (pH 7.6), 150 mM NaCl]/0.1 % Tween 20 for 30 min in order to deactivate reactive surface groups, washed two times in 1x PBS and dried using compressed air. The chips were mounted to the FAST frame multiwell chambers (Whatman Ltd. GB) to create 16 array fields.

Figure 18: Whatman Frame System (www.whatman.com)

All incubation steps were carried out on the orbital shaker (Stovall) at room temperature and slides were washed three times in PBS (pH 7.2)/0.1 % Tween 20 (“PBST”).

A calibration curve was set up for biomarker quantification. To do so, the chip was incubated with serial dilutions of antigen standards diluted with a solution of assay buffer j [0.1 M Tris (pH 7.4), 10 mM $CaCl_2$, 100 mM NaCl, 0.1 % Tween 20] and CRP-free Hytest serum in a ratio of 1:10.

An incubation time of 2.5 hours was chosen as longer incubation times are needed for equilibrium, especially when the analyte concentration is low, due to mass-transport

limitations. Furthermore lower incubation times lead to an increase in the limits of detection (LOD) and coefficients of variation [46].

A sample volume of 50 µL per well was added and incubated for 2.5 hours; working with a 1:10 sample dilution to reduce sample matrix effects [47] and four replicates (resulting in a set of 12 spots), 20 µL of patient serum are needed for the diagnostic test. After removing the sample solution and washing the slides in PBST, biotinylated detection antibodies with end concentrations of 1 µg/mL each were incubated for 1 hour, followed by an incubation step with labeled streptavidin (2 µg/mL streptavidin-Dy647, 4 µg/mL streptavidin-alkaline phosphatase, 4 µg/mL streptavidin-horse radish peroxidase, 100x dilution of streptavidin-horse radish peroxidase polymer, 10x dilution of streptavidin-gold nanoparticles) for 1 hour. Arrays processed with streptavidin-Dy647 were then washed two times in PBS and dried with compressed air. Arrays processed with streptavidin labeled alkaline phosphatase ("AP") were incubated with BCIP/NBT for 10 minutes. Arrays processed with strp-horseradish peroxidase ("HRP") or horse radish peroxidase polymer ("HRPp" in PBS/0.05 % Tween 20) were incubated with Diaminobenzidine ("dab") (incubation time: up to 30 minutes) or tetrametylbenzidine ("tmb") (incubation time: 30 minutes) as substrates. All substrates were purchased ready to use and added to the array according to the manual of the manufacturer.

The antigen-antibody complex was also detected with 40 nm gold particle labeled streptavidin ("strp-AuNP"). The stock solution of strp-AuNP was diluted 1:10 with a solution of 5 mg/mL bovine serum albumin in 0.15 M NaCl, 0.01 sodium phosphate (pH 7.0) and 0.05 % Tween 20. The slides were washed in 0.05 M aqueous EDTA for five minutes. The bound nanoparticles were then enlarged with a 1:1 Mix of 0.4 mM $HAuCl_4$ and 0.01 % NH_2OH*HCl for 3 minutes at room temperature ("hydroxylamine seeding" according to [48]). The particles were visualized through silver staining (a mixture of silver nitrate and hydroquinone) with the silver staining kit of Sigma (Austria).

7.2.4 Detection and data analysis

Fluorescence measurements (λ_{ex}=635nm, λ_{em}=670 nm) were performed using the Genepix 4000B non-confocal scanner (Axon Instruments, USA). The PMT gain, which is the amplification factor of the photomultiplier tube, was adapted to the signal intensity of the probes.

Colorimetric measurements were performed using Nikon 3000D, a customary digital camera for non-transparent slides or Clondiag ArrayMate (Germany), for transparent slides. The pictures were modified in Adobe Photoshop CS 5 (Inversion of colors, 16 bit grayscale and conversion to .tif) to allow analysis with Genepix 6.0 and therefore, comparison with the fluorescence data.

The fluorescence data and the processed pictures of the colorimetric slides were aligned according to the respective .gal files and analyzed generating .gpr files. Twelve spots were summarized to a set; the intensities of these spots were averaged, background corrected and evaluated by their mean standard deviation ('std'); the reproducibility is defined by the coefficient of variation ('CV'). Calibration curves were fitted using the growth sigmoidal fit of GraphPad Prism 5.0 or Origin Pro 7.5. The limit of detection (LOD) was calculated as the concentration corresponding to the intensity of the blank + 3 times standard deviation of the blank; the limit of quantification (LOQ) was calculated as the concentration corresponding to the intensity of the blank + 10 standard deviations of the blank.

8 Results and Discussion

8.1 Scheme of detection principles

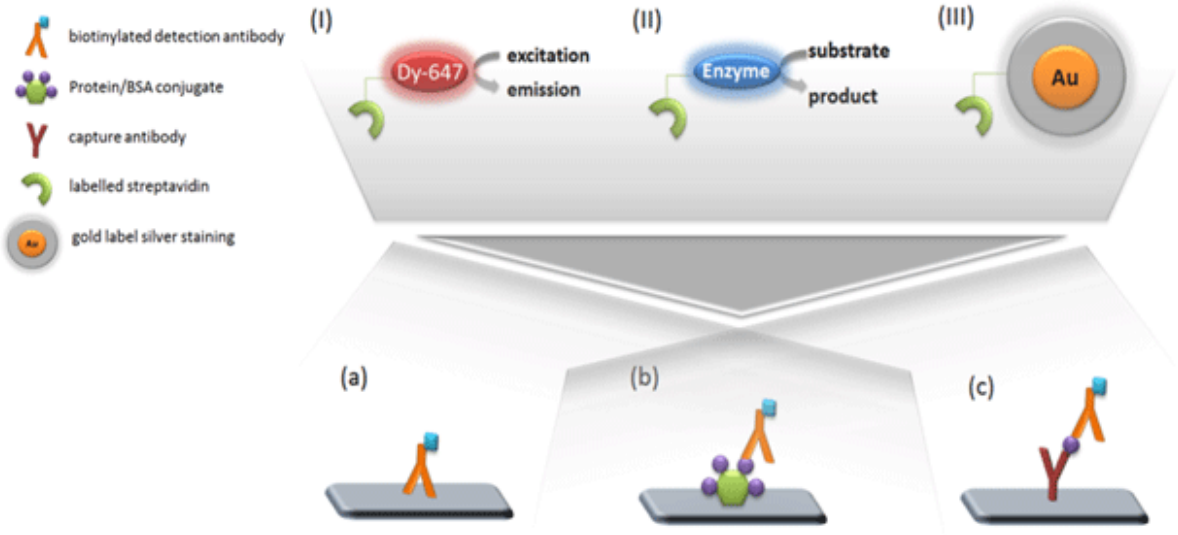

Figure 19: Scheme of on-chip assays using (I) fluorescence detection, (II) enzymatic detection, and (III) gold label silver staining

Different colorimetric detection principles as depicted in (Figure 19, (II) and (III)) were compared to conventional fluorescence-based read-out (Figure 19, (I)) with respect to assay sensitivity, reproducibility of measurement and assay time including the parameters limit of detection (LOD), limit of quantification (LOQ) and coefficient of variation (CV). In addition, different chip substrates (ARChip Epoxy, Slides with Nitrocellulose, PVDF and Nyloncoating) were evaluated.

Thereby the complexity of the on-chip immunoassay was increased from a direct immunoassay with immobilized a) antibody and b) BSA/antigen conjugate to c) a sandwich immunoassay.

The “direct assay” with spotted biotinylated antibodies (Figure 19 (a)) was the shortest assay (1 to 1.5 h) of the three tested ones as it was completed upon addition of labeled streptavidin within one reaction step. This assay principle was mainly used to compare the three different chip substrates.

The array with spotted BSA/antigen conjugate (Figure 19 (b)) was processed with biotinylated antibody and labeled streptavidin. The assay time was 2.5 hours. This principle was used for the optimization steps.

The sandwich assay format (c) was used for quantification of IL-8 and S-100 in serum: the antibody was immobilized to capture the analyte of interest which was then detected with biotinylated secondary antibody and labeled streptavidin. CRP was quantified in a binding inhibition assay as reported in [5].

8.2 Detection via Alkaline Phosphatase

Colorimetric assays with spotted S-100/BSA conjugates and biotinylated anti S-100 were performed to test various chip surfaces, blocking methods, assay buffers and furthermore, optimize the AP-streptavidin concentration.

8.2.1 Evaluation of chip substrates

8.2.1.1 Comparison of transparent slides

To study the effect of different substrate materials (polymer, glass) and surface chemistries (aldehydesilane, epoxysilane and SU-8) on the colorimetric detection with alkaline phosphatase a set of transparent polymer slides (Permanox, Zeonex) and glass substrates (ARChip Epoxy, Schott Nexterion) was defined and evaluated using the direct assay as introduced in section 8.1. Figure 20 shows a comparison of the absorbance signals obtained with the various surfaces. From the Figure it´s obvious that all tested slides perform equally well. In our experiments, ARChip Epoxy was further used.

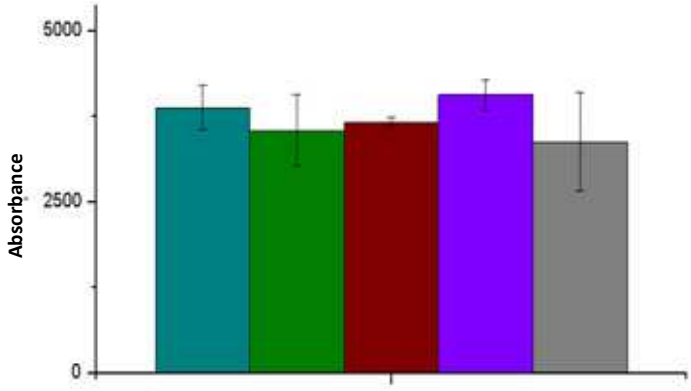

Figure 20: Spot intensities for ARChip Epoxy (blue), Permanox® (green), Slide AL (red), Slide E (purple) and spincoated Zeonex SU-8 (grey) for 0.3 µg/mL spotted biot. a-S100 (right), processed with 4 µg/mL strp-AP. Read out with Clondiag ArrayMate.

8.2.1.2 Comparison of transparent ARChip Epoxy with non-transparent slides

Slides with three different surface chemistries (ARChip Epoxy, SuperNitro and SuperPVDF) were compared in a direct assay as presented in 8.1 (a). Transparent slides were scanned with Clondiag ArrayMate, while non-transparent slides were read out with Nikon 3000D.

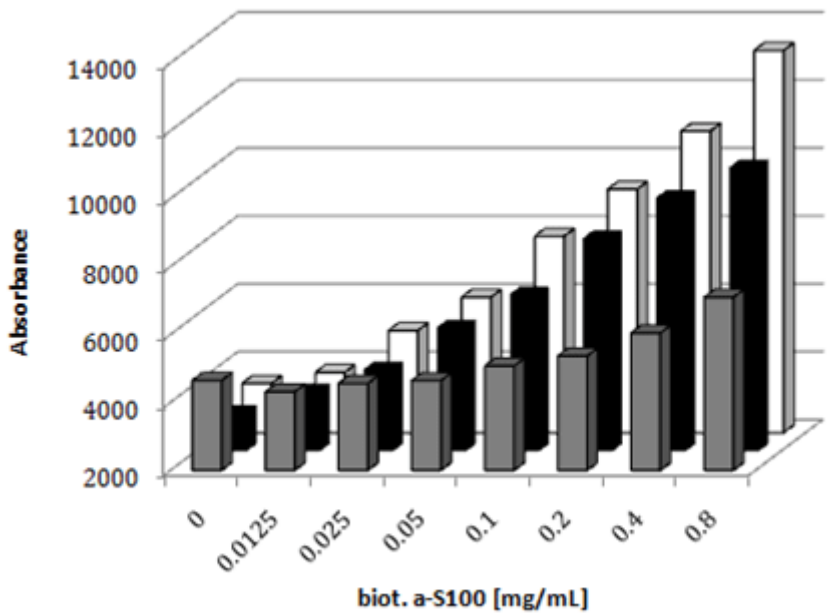

Figure 21: Direct assay of spotted biotinylated S-100 antibodies on ARChip Epoxy (grey), PVDF (black) and Nitrocellulose slides (white) using ap detection.

Nitrocellulose slides showed highest signals, slightly higher than PVDF slides, but nearly two times enhanced compared with ARChip Epoxy. Reproducibility of results was comparable for ARChip Epoxy (CV 8.9 %) and SuperNitro (CV 9.3 %), but inferior for PVDF slides (CV 14.5 %).

The lower sensitivity using ARChip Epoxy might be due to the flat, non-porous surface and therefore low capacity to retain precipitating product [20]. PVDF membranes are known to not bind proteins completely, depending on the protein 10 to 50 % is passing through the membrane [49] and therefore show lower signal intensities. In general, different surface architectures result in different efficiencies in chromogenic precipitation. According to the results of Le-Goff et al. (2012), the immobilization substrate has a great impact on the signal intensity, leading to increased signal intensity with more porous surfaces [20]. Also Petersen et al. (2007) reported that porous surfaces show higher signal intensities in colorimetric detection [24]. Nitrocellulose provides a three-dimensional matrix into which molecules can attach, the three-dimensional nature of the coating provides a much greater binding capacity than two-dimensional surfaces [25]. The high binding capacities result in high surface areas and probe densities [20].

Clearly, nitrocellulose slides were superior over ARChip Epoxy and PVDF in terms of signal strength, assay sensitivity and reproducibility of results and thus used for further experiments.

8.2.1.3 Effect of chip substrate on colorimetric and fluorescence detection

Requirements for chip surfaces employed in colorimetric and fluorescence detection schemes are completely different. While transparent glass slides are more suitable for fluorescence detection as they show low background fluorescence and allow detection with transmitted light, slides modified with membranes are more suitable for colorimetric detection as the white background results in higher contrast and more sensitive detection. Therefore, membranes are the gold standard support for enzymatic colorimetry-based methods involving precipitating substrates [20].

To study the effect of transparent and non-transparent slides on colorimetric and fluorescence-based assays, assay (b) (section 8.1) was performed in combination with either strp-Dy647 or strp-AP.

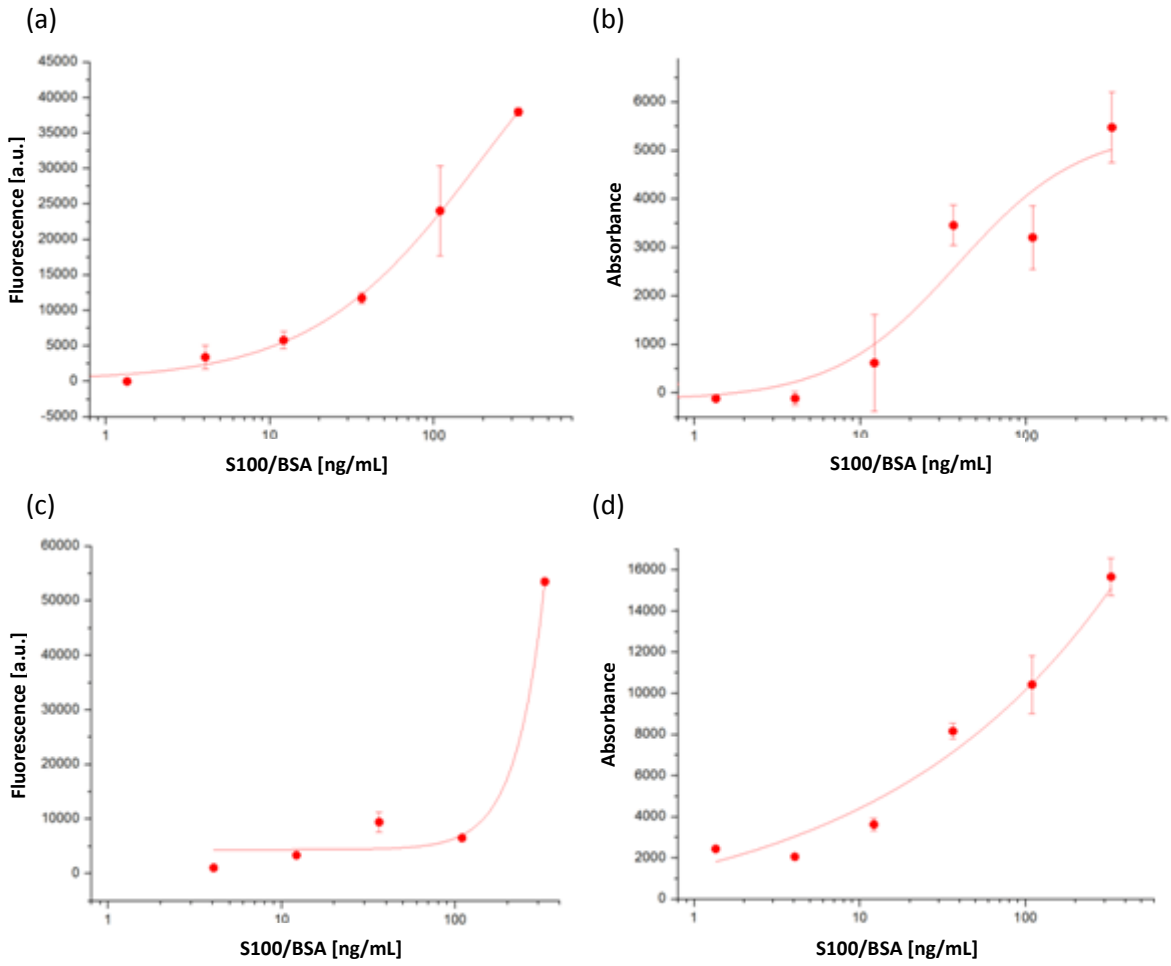

Figure 22: Effect of surfaces on detection with strp-dy647 and strp-AP. (a) fluorescence detection on ARChip Epoxy (read-out with Genepix 4000B) (b) AP detection on ARChip Epoxy (read-out with Clondiag ArrayMate) (c) fluorescence detection on Nitrocellulose surface (read-out with Genepix 4000B) (d) AP detection on nitrocellulose surface (read-out with Nikon 3000D).

Figure 22 shows the respective calibration curves. ARChip Epoxy processed with strp-Dy647 shows a dynamic range of 4 to 300 ng/mL S-100/BSA, whereas processed with

strp-AP a dynamic range of 30 to 300 ng/mL S-100/BSA. Nitrocellulose slides in combination with fluorescence detection result in smaller dynamic ranges (100 to 300 ng/mL S-100/BSA) and increased LOD's (up to factor 10).

Using nitrocellulose slides withcolorimetric detection a 10 times lower LOD is reached than with fluorescence detection. Though the assay performance is similar to that of ARChip Epoxy, assay sensitivity represented by the slope of the curve is enhanced, and reproducibility given by the coefficient of variation (CV) is clearly improved (8 % on nitrocellulose vs. 15 % on ARChip Epoxy), according to the results in Figure 22, the signal intensity is more than doubled in colorimetric detection using nitrocellulose as chip substrate.

Nitrocellulose is more suitable for colorimetric detection methods as the chromogenic precipitate is more visible on the white background and the 3D structure provides higher binding capacities [25]. The decrease in dynamic range for fluorescence detection is a result of the optical properties of nitrocellulose, nitrocellulose is not intrinsically fluorescent, but it reflects light as white surfaces reflect all colors in the visible spectrum, including laser light from microarray scanners [50].

These results indicate that ARChip Epoxy is more suitable for fluorescence detection, whereas slides with nitrocellulose surface have a positive effect on signal progression in detection with AP.

8.2.2 Optimization of blocking methods

Unoccupied binding sites need to be blocked to minimize background signals caused by unspecific binding [51]. The appropriate blocking protocol depends on the chip surface and the assay architecture. For ARChip Epoxy Slides, the blocking solution was reported previously [46], [10]: the slides were incubated in 1x PBS (pH 7.2)/0.1% Tween 20 for 30 min. For blocking of the nitrocellulose slides 1x PBS (pH 7.2) or 1x TBS containing Tween 20 and optional 1-6 % milk powder were used as recommended by the manufacturer. Therefore, these three blocking buffers were tested using assay (b) as described in 8.1 (S100/BSA was spotted and the chip incubated with biotinylated a-S100, strp-AP and BCIP/NBT).

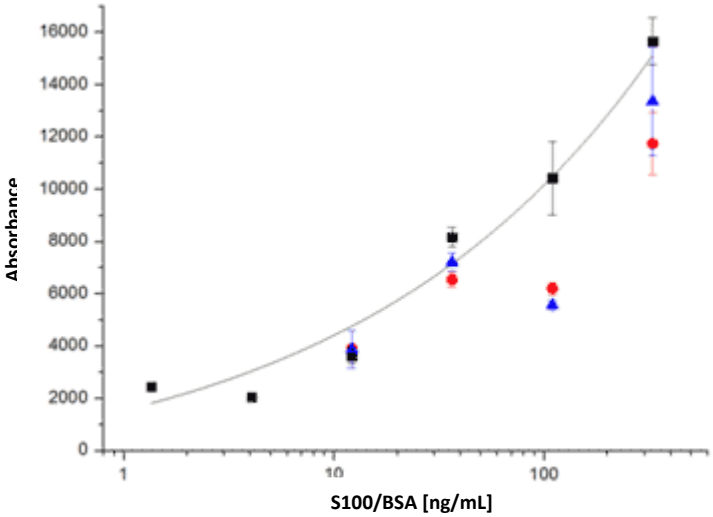

Figure 23: Calibration curve using different blocking solutions (black: 1x PBS (pH 7.2)/0.1% Tween 20 “PBST”, red: 1x TBS (pH 7.4)/0.1% Tween 20 “TBST”, blue: 1x TBS (pH 7.4)/0.1% Tween 20+3% milk powder “TBST+MP”). The chips were processed using 4 µg/mL Strp-AP. Curve fit: growth/sigmoidal of Origin 7.5.

Figure 23 shows the respective calibration curves indicating that the choice of blocking buffer has no great impact on the assay performance. The mean coefficients of variations differ minimally (PBST: 7.9 %, TBST: 6.0 %, TBST+MP: 7.8 %). However in arrays blocked with PBST 67 % of all 10 ng/mL to 300 ng/mL S100/BSA spots were available for data analysis, while in arrays blocked with TBST and TBST+MP only 44 % and 59 % of processed spots could be analyzed. This corresponds well to the results of [52] where PBST without supplements is described as standard blocking reagent for nitrocellulose slides. As a result, PBST was used as blocking buffer in further experiments.

8.2.3 Test of assay buffer

The assay buffer, often supplemented with stabilizing agents, plays an important role in microarrays. It ensures suitable binding conditions, such as proper pH and ionic strength during the immunoreactions [51]. Various companies offer assay buffers that promise less cross reactivity, higher signal intensities and lower backgrounds than conventional buffer compositions.

In order to evaluate the effect of different buffer compositions on colorimetric detection with alkaline phosphatase, three assay buffers, of which two were commercial, were compared using a direct assay as schematically shown in Fig. 1 (a): SD1 General Sample Diluent “SD1” and HISPEC Assay Diluent “Buf049A” of unknown composition were compared to buffer j in terms of signal intensity.

Buffer j was chosen as in previous studies it worked best with respect to [46][46][46][45]data reproducibility, slope and linearity of the calibration curve [46]. SD1 and Buf049A were included because preliminary tests with fluorescent detection revealed slightly lower off-set than with buffer j (see Figure 24).

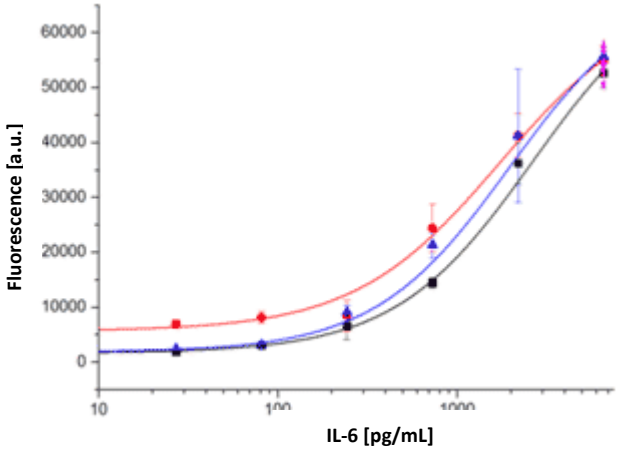

Figure 24: Curve fit of sandwich assay for IL-6 processed with red: buffer j, blue: SD1 and black: Buf049A. Read-out with Genepix 4000B and curve fits in Origin Pro 8.5.

Figure 25: Images of arrays processed with 2 µg/mL strp-AP in buffer J using ARChip Epoxy. Pictures were taken in Clondiag ArrayMate.

As is obvious from Figure 25 and in contrast to the results presented in Figure 24, only arrays processed with buffer j show visible spots in colorimetric detection. No results were obtained using assay buffers SD1 and Buf049A. The high signal intensities achieved with buffer j might be due to its chemical composition. In contrast to PBS systems or buffers containing EDTA, Tris buffers do not inhibit the phosphatase activity, therefore, Tris buffers are commonly used for alkaline phosphatase detection [53]. Therefore assay buffer j was used in further experiments.

8.2.4 Optimization of streptavidin concentration

The concentration of AP-labeled streptavidin (strp-AP) and therefore, amount of potentially binding enzyme has critical influence on the signal progression. Thus, different concentrations of AP-labeled streptavidin (2, 4 and 8 µg/mL) were tested to study the effect of streptavidin-AP on signal intensity and assay performance. 0 to

328 ng/mL S-100/BSA was spotted on ARChip Epoxy Slides incubated with biotinylated a-S100, strp-AP and BCIP/NBT as substrate. The slides were scanned in Clondiag ArrayMate and curve fits were created in Origin Pro 7.5 as plotted in Figure 26.

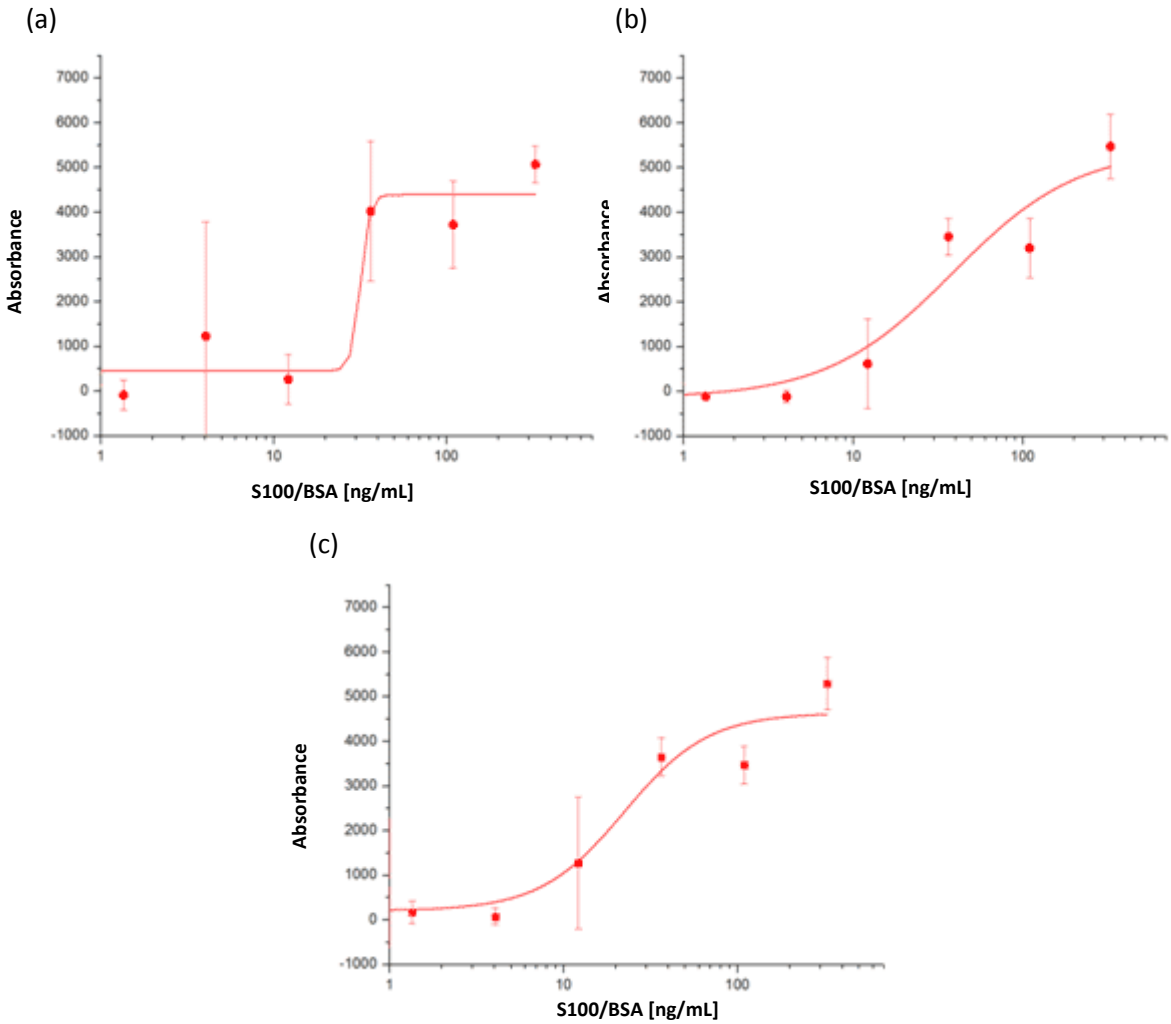

Figure 26: Curve fits for 0 ng/mL to 328 ng/mL S100/BSA processed with (a) 2 µg/mL strp-AP, (b) 4 µg/mL strp-AP, and (c) 8 µg/mL strp-AP. Curve fit: growth/sigmoidal of Origin 8.5.

As is obvious from the calibration curves the dynamic range increases with increasing AP-labeled streptavidin concentration: while the dynamic range using 2 µg/mL AP-strep is extremely short (20 to 30 ng/mL S100/BSA), the linear range is significantly enhanced with 4 and 8 µg/mL strp-AP (4 to 100 ng/mL S100/BSA). In addition, reproducibility given by the mean coefficient of variation (CV) is improved with increasing strp-AP concentration resulting in 24 %, 15 % and 12 % for 2, 4 and 8 µg/mL strp-AP. As 4 µg/mL and 8 µg/mL are comparable in performance and equally effective, 4 µg/mL strp-AP was used in further measurements.

8.3 Detection via Horseradish Peroxidase

Colorimetric assays with spotted S-100/BSA conjugates and biotinylated anti S-100 were performed to

- test various chip surfaces
- evaluate the use of horse radish peroxidase polymer
- optimize the AP-streptavidin concentration
- test different enzyme substrates and substrate compositions.

8.3.1 Evaluation of chip surfaces

0 to 0.8 mg/mL biot. a-S100 (8.1, (a)) was spotted on ARChip Epoxy, PVDF and Nitrocellulose slides to evaluate the most appropriate chip surface for detection with horseradish peroxidase polymer (HRPp).

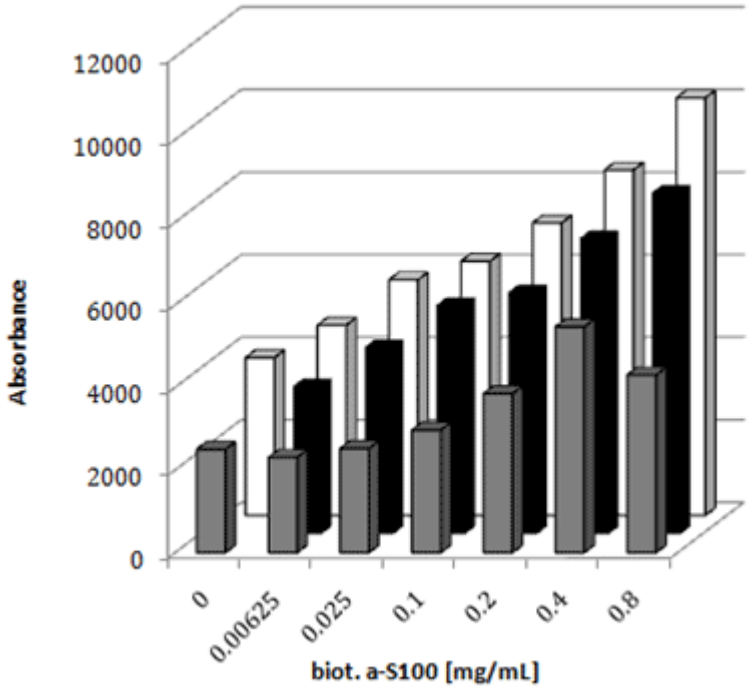

Figure 27: Direct assay of spotted biotinylated S-100 antibodies on ARChip Epoxy (grey), PVDF (black) and Nitrocellulose slides (white) using strp-HRPp detection. Read-out with Clondiag ArrayMate (ARChip Epoxy) and Nikon 3000d (PVDF and Nitrocellulose).

As can be seen from Figure 27 nitrocellulose slides are the chip surfaces of choice for colorimetric measurement via HRPp. PVDF shows slightly decreased signals, while the signals on ARChip Epoxy are reduced by 50 %. This is in good agreement with the results obtained for alkaline phosphatase plotted in Figure 21. As Nitrocellulose is a three-dimensional porous network with a high surface area and is linked with higher

probe density, spotted volume is completely adsorbed due to capillary forces, leading to larger spot sizes and easier optical read-out [20]. PVDF showed higher background signals corresponding to the results of [54], the background correction of the data results therefore in lower signal intensities as can be observed in Figure 27. The mean coefficient of variation over all biot.a-S100 concentrations is 12 % for SuperNitro, 29 % for SuperPVDF and 17 % for ARChip Epoxy. Summing up, Nitrocellulose coated slides are most suitable for detection with strp-HRPp among the tested materials.

8.3.2 HRP versus HRP polymer

Horse radish peroxidase (HRP) and horse radish peroxidase polymer ("HRPp")-labelled streptavidin was compared using the colorimetric assay (b) (see section 8.1). HRPp is produced by covalently conjugating streptavidin with horse radish peroxidase to a hydrophilic polymer backbone. According to the manufacturer, the multiple biomolecules increase the biotin binding capacity and amplify the enzyme. For the test, a 100x dilution of strp-HRPp stock (1 mg/mL) and 4 µg/mL HRP were used.

Figure 28: ARChip Epoxy spotted with S-100/BSA and processed with biotinylated antibody and a 100x dilution of strp-HRPp. Read-out with Clondiag ArrayMate.

Figure 28 shows that the horseradish peroxidase polymer leads to visual spot development in contrast to the use of 4 µg/mL strp-HRP which did not lead to detectable results. The use of peroxidase polymer increases signal intensity and therefore, facilitates the data analysis which is in good correspondence to the results of [55], who compared the signal intensities of different dilutions of strp-HRP and strp-HRPp leading to the result that the signal intensities for strp-HRPp were doubled. Strp-HRPp is thus used for further experiments.

8.3.3 Optimization of HRPp-streptavidin concentration

A 100x, 200x and 1000x dilution of HRPp labeled streptavidin was tested using assay (b) as described in section 8.1. Evaluation criteria were the dynamic range, reproducibility of results (% CV) and fluorescence signal.

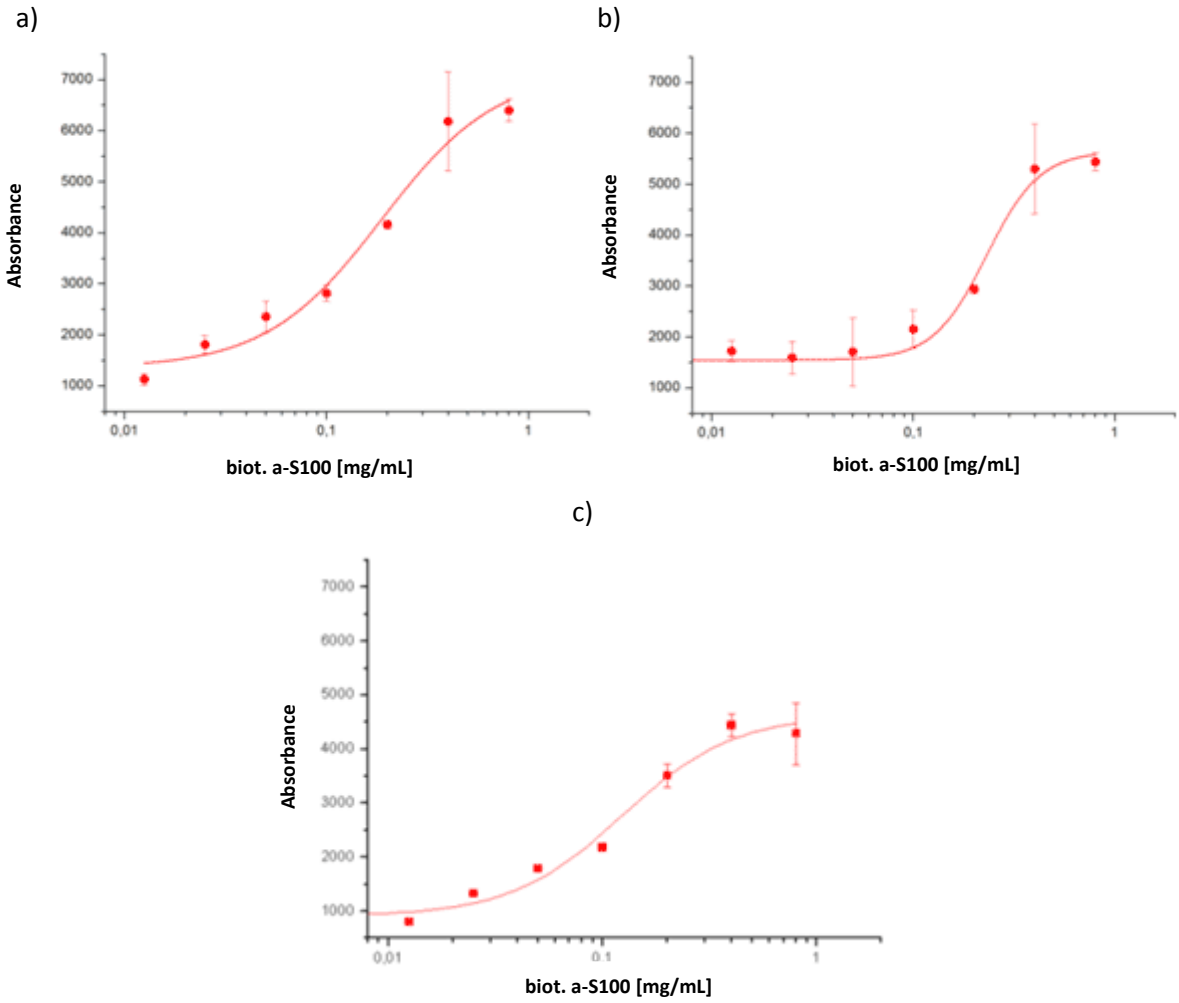

Figure 29: Comparison of the biot. a-S100 calibration curve processed with a) 100x dilution b) 200x dilution c) 1000x dilution of HRPp labeled streptavidin and dab with 0.03 % $NiCl_2*H_2O$ as substrate. Read out with Clondiag ArrayMate.

Figure 29 indicates that HRPp signal intensities are similar for 100x and 200x dilution, but reduced by 30% with 1000x dilution of HRPp-labeled streptavidin. Clearly, varying the dilution factor of strp-HRPp in the assay allows to tune the dynamic range of the curve. Considering both signal intensity and dynamic range 100x dilution leads to the best assay performance. Especially when adding 0.03 % $NiCl_2*H_2O$ greater assay sensitivity (Figure 29) and improved data reproducibility was achieved as shown in Table 1 (page 45).

8.3.4 Enzyme substrates

3,3'-diamonobenzidine solution ("dab") and 3,3',5'5-tetramethylbenzidine liquid substrate ("tmb") are widely used enzyme substrates for colorimetric measurement with HRP. Tmb, which forms the blue 3,3',5'5-tetramethylbenzidine diimine when oxidized, was successfully used in the colorimetric microarrays of [1], whereas

according to [31], Diaminobenzidine (dab) is the substrate for most sensitive detection with HRP. The dab precipitate is stable and produces an intense signal with relatively low background, tmb is non-carcinogenic and non-mutagenic but may require increased washing and blocking due to higher background staining [56].

To compare the two substrates in the present architecture, S-100/BSA conjugates, biot. antibodies and capture antibodies for S-100 were spotted on slides with nitrocellulose surface.

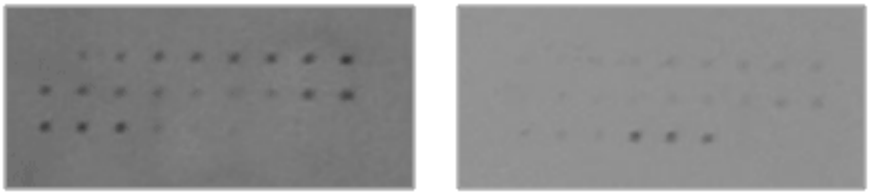

Figure 30: Array processed with S-100, 1 µg biot. a-S100 and 100x dilution of strp-HRPp on SuperNitro, left: with dab as substrate, right: with tmb as substrate. Read out with Nikon 3000d.

Figure 30 presents images of arrays processed with the two different enzyme substrates. It can be seen that arrays processed with dab show darker spots than arrays processed with tmb. According to [57] using dab as substrate results in higher signal-to-noise ratios, which also was confirmed in this experiment: the signal-to-noise ratio is increased by 25 %. Therefore, dab was considered more appropriate for this application; it was thus used for further measurements.

8.3.5 Optimization of substrate composition

The staining sensitivity of spots processed with dab can be enhanced by the addition of Ni^{2+} or Co^{2+}, then the color of the precipitate changes from brown to black/blue-black. Therefore, not only the stain intensity is increased, but also the contrast between stains and background.

To do so, ARChip Epoxy slides were spotted with biot. a-S100, incubated with strp-HRPp and dab as substrate containing Nickel(II)chloride hexahydrate in a concentration of 0.03 % (w/v) as recommended by the manufacturer. The arrays were analyzed in Genepix 6.0 and curve fits were created in Origin Pro 7.5. to compare signal progression and coefficients of variation.

Figure 31 shows curve fits of arrays processed with dab with and without 0.03 % $NiCl_2*6H_2O$. As is obvious from the figure, the dynamic range of the curves is similar, while the assay sensitivity defined by the slope of the curve is significantly enhanced

upon addition of $NiCl_2*6H_2O$. Data reproducibility was also improved (Table 1). In conclusion, dab containing 0.03 % $NiCl_2*6H_2O$ was used as enzyme substrate for further measurements.

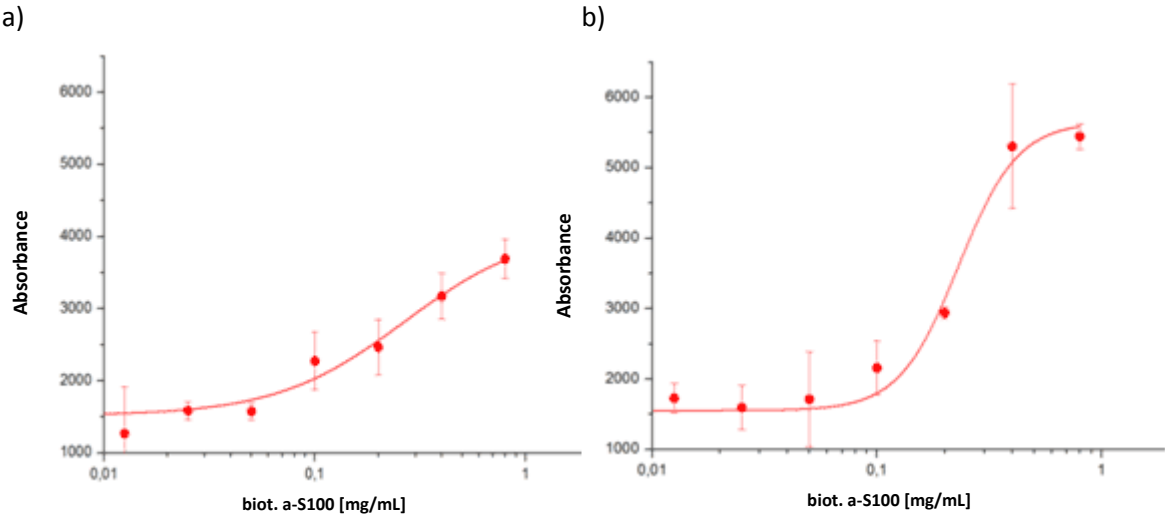

Figure 31: Comparison of the biot. a-S100 calibration curve detected via HRPp labeled streptavidin and dab a) without and b) with 0.03 % $NiCl_2$ * 6 H_2O. Read-out with Clondiag ArrayMate.

Table 1: Mean coefficients of variation of the biot. a-S100 calibration curve obtained with different dilutions of horse radish peroxidase polymer labeled streptavidin (strp-HRPp)

strp-HRPp dilution	dab	0.03% $NiCl_2*6H_2O$ in dab
100x	15%	6%
200x	17%	12%
1000x	5%	6%

8.4 Detection using Au Nanoparticles

Gold nanoparticles and silver staining for the detection in microarrays was reported to show comparable sensitivity to fluorescent detection [20-22]. In order to adapt this detection method to the current assay architecture, colorimetric assays with spotted S-100/BSA conjugates and biotinylated anti S-100 were performed. Various chip surfaces were tested and assay conditions (assay buffer, streptavidin concentration, washing) were optimized. In addition, particle size of Au nanoparticles and the use of the hydroxylamine seeding method was evaluated as reported in [48].

8.4.1 Evaluation of chip substrates

To study the effect of different surface chemistries on the detection with AuNP, biot. a-S100 (according to section 8.1, (a)) was spotted on ARChip Epoxy, PVDF and Nitrocellulose slides.

No signals were obtained on three-dimensional PVDF and nitrocellulose surfaces. After silver staining, spot signals could not be differed from background as hydrophobic components of nitrocellulose and PVDF attract binding of the gold particles which results in non-specific binding [58].
By contrast, using transparent slides, such as ARChip Epoxy the drawbacks from silver staining as observed on porous membranes can be avoided.

8.4.2 Test of dilution buffer

The choice of diluting buffer for the strp-AuNP stock is of great importance to prevent aggregation and reduce unspecific binding of the gold nanoparticles. The manufacturer of strp-AuNP recommends dilution of the strp-AuNP stock in a buffer of pH 6 to 8 containing 0.15 M saline plus 0.5 % albumin and 0.05 % Tween 20 (“dilution buffer gold”) to reduce background signals. This buffer was compared with standard assay buffer j using assay (b) as described in section 8.1 on ARChip Epoxy.

Figure 32 shows the curve fit of the arrays processed with dilution buffer, no results were obtained using buffer j: only 25 % of the spots could be analyzed, these showed weak signals and no correlation to the spotted antigen concentration. The use of dilution buffer gold results in higher signal intensities as albumin can effectively block the nonspecific surface adsorption of free Au nanoparticles [59]. Therefore, strp-AuNP was diluted in dilution buffer gold in further measurements.

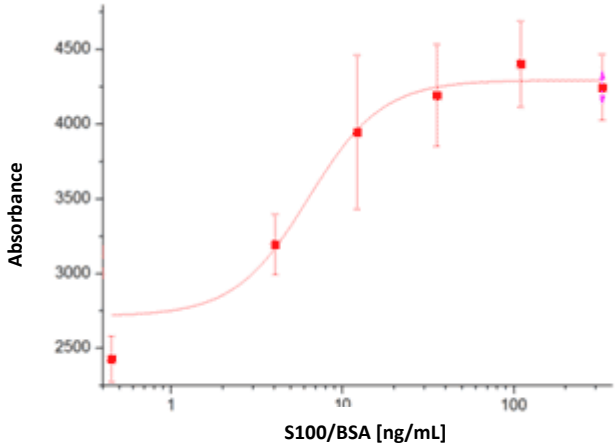

Figure 32: Curve fit of Arrays spotted with S-100/BSA and processed with 10 x dilution of strp-Au in dilution buffer gold. Scanned with ClonDiag Arraymate.

8.4.3 Optimization of streptavidin concentration

The concentration of strp-AuNP and therefore, the amount of added gold nanoparticles has critical influence on the signal intensity and signal progression. Strp-AuNP dilutions ranging from 1:5 up to 1:100 are recommended by the manufacturer. Thus, arrays were processed with 10x, 50x and 100x dilution of strp-AuNPs using ARChip Epoxy. The respective curve fits are presented in Figure 33.

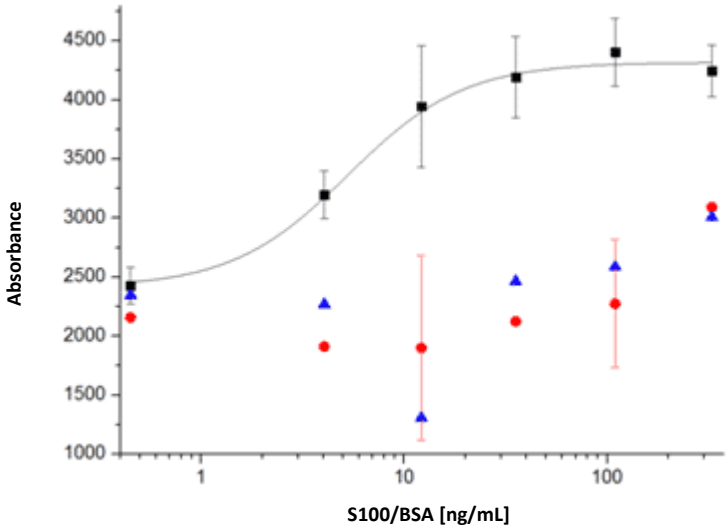

Figure 33: Calibration curve using different dilutions of strp-AuNP in dilution buffer gold (black: 10x dilution, red: 50x dilution, blue: 100x dilution)

Figure 33 indicates that the concentration of strp-AuNP has indeed great impact on the assay performance. In arrays processed with 1:50 or 1:100 dilution of Strp-AuNP only 22 % of all spots could be analyzed and the signals do not correlate with the spotted

antigen concentration. Arrays processed with 10x dilution of strp-AuNP show higher signal intensities, more than 80 % of all spots could be used for data analysis. Thus a dilution of 1:10 was used for further experiments.

8.4.4 Optimization of washing conditions

Background signals can be a result of halides that cause a silver precipitation reaction; therefore the washing protocol before silver staining is critical. In order to reduce unspecific background signals, additional washing steps with aqueous 0.05 M EDTA for five minutes as recommended by [58] were evaluated. Before the silver staining process, the slides were washed in H_2O according to the recommendations of the manufacturer and additionally washed with and without 0.05 M EDTA for five minutes as EDTA is known to bind cations. ARChip Epoxy slides using assay (b) as described in section 8.1 were used to compare the results visually and to identify differences in background and signal intensity.

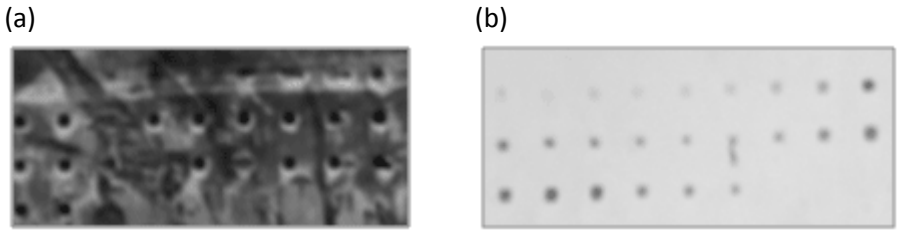

Figure 34: Comparison of wells processed with streptavidin-gold (40 nm particle size). a) washed in aqua dest. b) washed additionally with 0.05 M EDTA for 5 minutes Read out with Clondiag ArrayMate.

Figure 34 shows images of arrays washed with (a) aqua dest and (b) additionally with 0.05 M EDTA for 5 minutes before silver staining. A more stringent washing protocol with 0.05 aqueous EDTA reduced background signals by 83 % and was thus used for further measurements.

8.4.5 Effect of particle size and evaluation of hydroxylamine seeding

A key advantage of using gold nanoparticles in molecular biology is the availability of different particle sizes and therefore, the possibility to choose the particle size depending on the application. While smaller gold particles yield labelings of higher intensities and of better resolution, they also have the tendency of leading to higher background; on the other hand, the use of larger particles allows easy identification of labeled structures at low magnification but increased charge repulsion between larger particles may inhibit access to the target [59]. Therefore, particle diameters above

approximately 100 nm should be avoided [60]. According to the manufacturer, nanoparticles with a size greater than 15 nm are more suitable for light microscopy, whereas particle size smaller 15 nm are more suitable for TEM, indicating that larger particles are more promising for the current assay architecture.

In 2002 Zhanfang Ma and Sen-Fang Sui [48] reported a method to enlarge gold nanoparticles with a mixture of $HAuCl_4$ and $NH_2OH*HCl$; hydroxylamine catalyzes the reduction of Au^{3+} ions to bulk metal, this reduction is accelerated by gold surfaces. As a result, all added Au^{3+} ions go into production of larger particles which results in an increase of particle diameter of up to 36-fold [48]. Larger particles increase the precipitation of silver and therefore the signal intensity. Herein we tested if the treatment with $HAuCl_4$ and $NH_2OH*HCl$ ("hydroxylamine seeding") increases the assay sensitivity and reproducibility in the current assay architecture.

In order to evaluate the gold particle size and the hydroxylamine seeding method, 10 nm, 20 nm and 40 nm gold nanoparticles with and without hydroxylamine seeding were compared with respect to reproducibility and sensitivity. S-100/BSA conjugates were spotted on ARChip Epoxy slides and processed using assay (a) as described in section 8.1. The data of the arrays was plotted in Origin Pro 7.5.

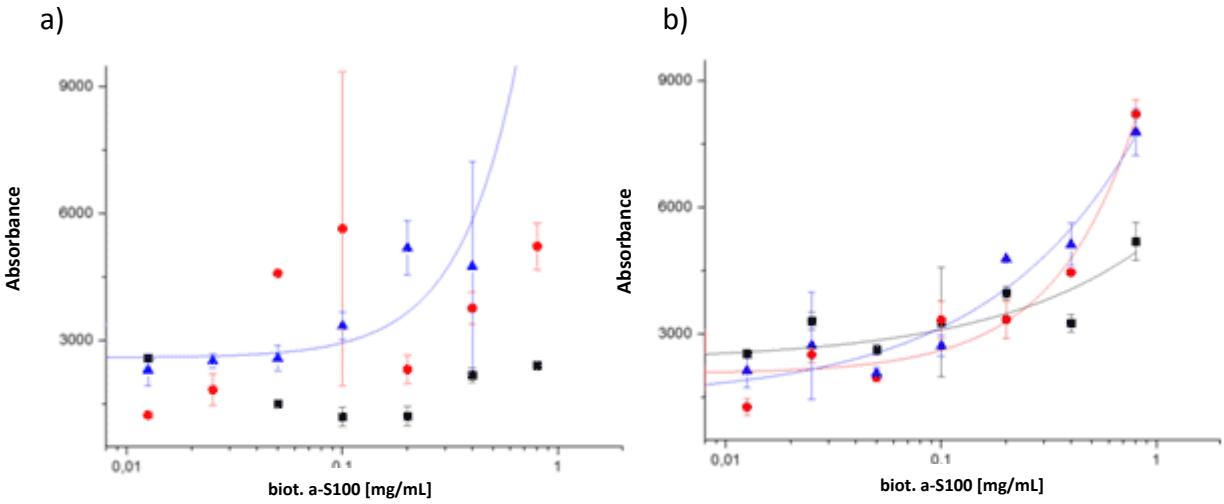

Figure 35: Biot. a-S100 calibration curve processed with a) AuNP labeled streptavidin and b) AuNP labeled streptavidin with hydroxylamine seeding. Black: 10 nm particle size, red: 20 nm particle size, blue: 40 nm particle size. Read out with Clondiag ArrayMate.

Figure 35 a) shows calibration curves of the arrays processed with strep-Au nanoparticles of different size; arrays processed with the largest strep-Au particles (40 nm) show highest sensitivity defined by the slope of the curve. This results correspond to [61]: Choi et al. (2010) tested different gold particle sizes and found for a gold particle size of 40 nm highest colorimetric signal intensities, size diameters > 40 nm

resulted in lower intensities because of steric hindrances [61]. As can be seen in Figure 35 b) the use of hydroxylamine seeding resulted in slightly smaller standard deviations (12 % with hydroxylamine seeding, 16 % without at a AuNP diameter of 40 nm) and the dynamic range was enlarged by one order of magnitude (0.05 mg/mL up to 0.8 mg/mL biot. a-S100 vs. 0.2 mg/mL up to 0.8 mg/mL biot. a-S100 without hydroxylamine seeding). Among the compared assay architectures, 40 nm particle size with hydroxylamine seeding showed best results with regard to low coefficients of variation and large dynamic ranges.

8.5 Comparison of the colorimetric methods

The three colorimetric methods as described in 8.2, 8.3 and 8.4 were compared using ARChip Epoxy and nitrocellulose slides as chip substrates. While assay (b) (section 8.1) was used for method evaluation on ARChip Epoxy, assay (a) (section 8.1) was chosen for evaluation with nitrocellulose slides.

Figure 36 shows the normalized calibration curves obtained for ARChip Epoxy.

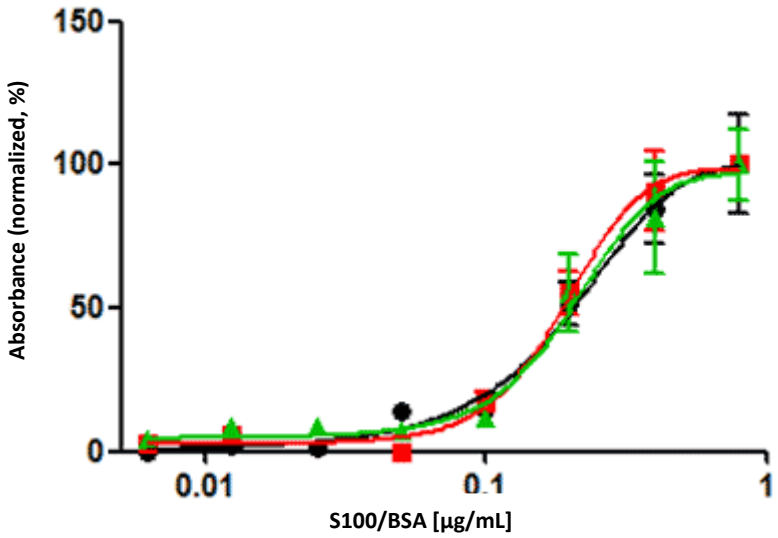

Figure 36: Calibration curves for S-100/BSA conjugates on ARChip Epoxy Slides comparing the detection methods AP (black), HRPp (red) and AuNP after hydroxylamine seeding and silver staining (green); for data comparison Y-values are normalized to a common scale. Read-out with Clondiag ArrayMate.

Normalized data demonstrate that the tested methods perform equally well as the sensitivity defined by the slope of the curve and the dynamic range covering 0.05 to 1 µg/mL S100/BSA are very similar for all detection methods. AP, HRPp and AuNP-based colorimetric detection methods were also compared with respect to the analytical parameters listed in Table 2, which indicate that the assay with AP detection is superior as it is faster and permits lower LOD and LOQ.

Table 2: Figures of merit for the calibration curve shown in Figure 36 using AP, Au and HRPp detection

Parameter	AP	HRPp	AuNP
Assay time	5 h 10 min	5 h 30 min	5 h 45 min
LOD (µg/mL)	0.08	0.16	0.25
LOQ (µg/mL)	0.16	0.32	0.35
CV (%)	11	13	18

The assay steps of every method are described in 7.2.3. AP and HRPp detection require the same number of assay steps, whereas processing the slides with strp-gold

nanoparticles needs additional procedures such as hydroxylamine seeding, which needs the addition of toxic and cancerogenic substances such as $NH_2OH*HCl$ that require special handling and proper disposal, and silver staining, which is sensitive to sunlight and fluctuations in temperature and increases the susceptibility to handling errors.

Figure 37 compares the calibration curves obtained on nitrocellulose with strp-AP and strp-HRPp detection. The data was plotted in Graphpad Prism 5.0. According to section 8.4.1 the AuNP detection method was not included in the evaluation.

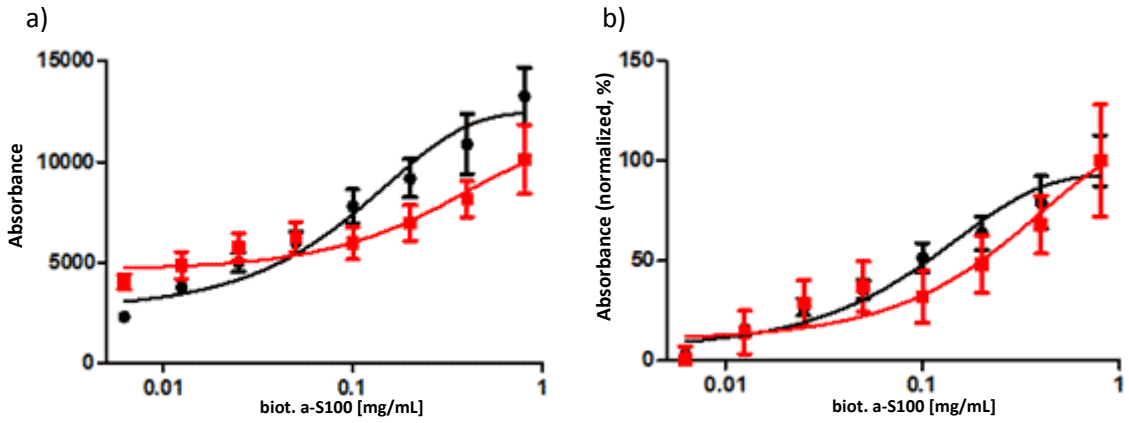

Figure 37: Biot. a-S100 calibration curve on nitrocellulose a) absolute intensities b) normalized values, processed with strp-AP (black) and strp-HRPp (red). Read out with Nikon 3000D.

Figure 37 a) demonstrates that arrays processed with strp-AP show up to 25 % increased signal intensities; the reproducibility defined by % CV is slightly improved in AP detection (9 % for strp-AP vs. 13 % for strp-HRPp).

When the Y-values are normalized to common scale (as can be seen in Figure 37 b)) the linear range in AP-detection is enhanced by one order of magnitude, ranging from 0.01 mg/mL to 0.5 mg/mL biot. a-S100 for strp-AP and compared with 0.1 mg/mL to 0.8 mg/mL biot. a-S100 for strp-HRPp.

As alkaline phosphatase detection performed best in terms of sensitivity, reproducibility and easy handling, it was used for multiplex quantification of IL-8 and S-100 in a sandwich and CRP in a binding inhibition assay.

8.6 Quantification of S-100, CRP and IL-8 with the final protocol

S-100 and IL-8 were determined via a sandwich assay (according to 8.1 (c)), whereas CRP was detected using a binding inhibition assay (as reported in [5]). The optimized colorimetric method was directly compared to fluorescence detection. All measurements were performed in spiked human serum diluted by factor 10 with assay buffer j.

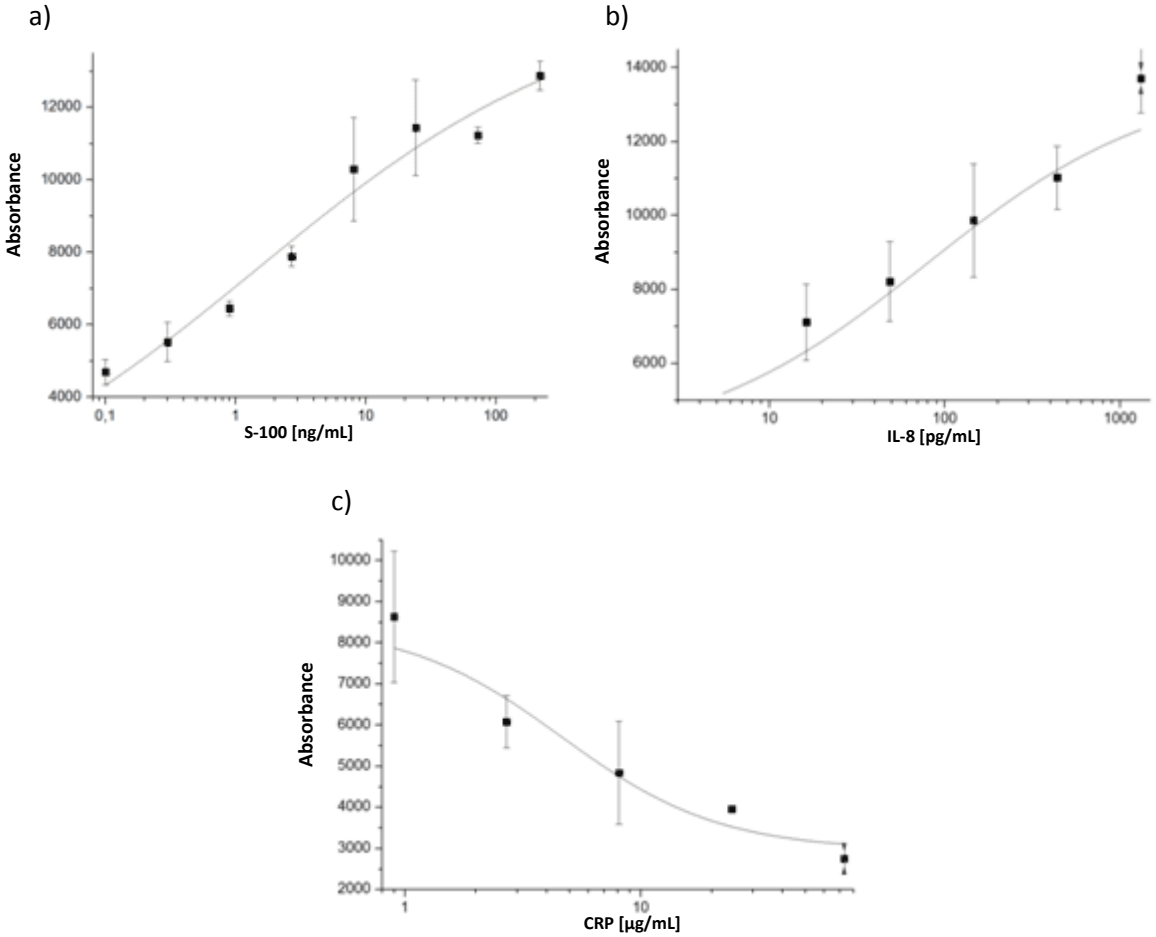

Figure 38: Calibration curves for a) S-100, b) IL-8 and c) CRP in spiked human serum (1:10 dilution) using AP detection.

Curve fits for AP-detection of S-100, IL-8 and CRP on nitrocellulose are presented in Figure 38. In contrast to the results of Wei et al. (2011) who found dynamic ranges covering two orders of magnitude in colorimetric detection with alkaline phosphatase of the tumor marker CEA on glass slides, colorimetric detection of S-100 on nitrocellulose leads to a dynamic range including three orders of magnitude (0.1 to 300 ng/mL S-100) [1]. The dynamic range of the sandwich assay for IL-8 covers 5 to 1000 pg/mL, the binding inhibition assay for CRP covers 1 to 100 µg/mL and therefore including two orders of magnitude. Cut-off values of the analytes were reported in 6.1 (IL-8: 20 pg/mL, CRP: 10 µg/mL, S-100: 10.4 ng/mL). Taking the 10x serum dilution into account, the chip is particularly appropriate for detecting elevated levels of S-100 as

the cut-off value lies within the linear range. For quantification of CRP the patient sample needs to be less diluted before measurement. CRP, S-100 und IL-8 can be detected simultaneously by implementing capture antibodies with higher affinity or recognition elements such as polypeptide scaffolds with phosphocholine as binder molecules which allow adjustments of the binding affinity through modifications of the polypeptide [62]. Adaptations can also be made by tuning the antibody concentration. Quantification of IL-8 allows classification of the severity of sepsis, as both the cut-off value for severe sepsis (87 pg/mL) and for septic shock (693 pg/mL) perfectly match the linear range of the calibration curve.

In Figure 39 the images of nitrocellulose slides and ARChip Epoxy processed with strp-AP and strp-Dy647 are presented. The calibration curves for S-100 are depicted in Figure 40. As is obvious from both figures and was also previously reported in 8.2.1, the choice of chip substrate is crucial for reliable and sensitive biomarker detection and strongly depends on the detection method.

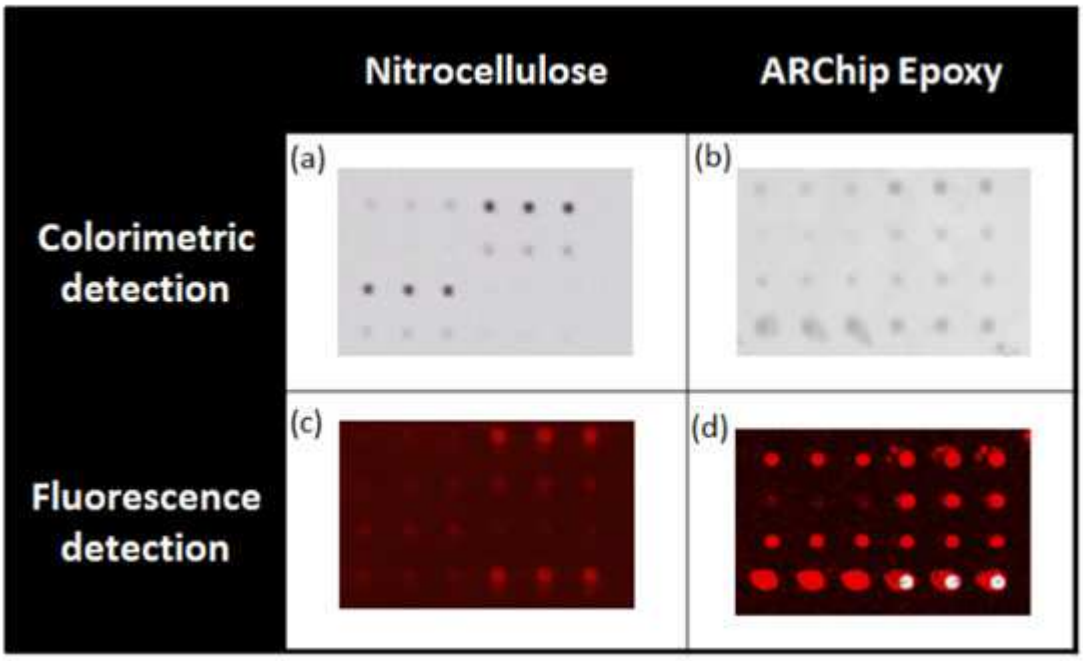

Figure 39: Images of arrays taken with Genepix 4000B (bottom left and right), Clondiag ArrayMate (top right) and Nikon 3000d (top left)

In fluorescence detection on ARChip Epoxy, the signal intensities increase fourfold compared to nitrocellulose slides. The background signals for nitrocellulose are five times enhanced compared with ARChip Epoxy, most probably because the membrane reflects laser light of the microarray scanner.

In colorimetric detection the reverse effect can be observed: signal intensities on nitrocellulose slides are two times enhanced compared with signal intensities on ARChip Epoxy as glass shows lower contrast and less capacity to retain the chromogenic precipitate. These results indicate that slides modified with nitrocellulose are the chip substrate of choice in AP detection.

Figure 40 shows standard curves for S-100 using strp-AP and strp-Dy647 for colorimetric and fluorescence detection. Using nitrocellulose slides and fluorescence detection, the linear range covers one order of magnitude (0.1 to 1 ng/mL S-100). For fluorescence detection on ARChip Epoxy the dynamic range is 0.3 ng/mL to 100 ng/mL S-100 which corresponds well to previous studies of Buchegger et al. (2011) and allows quantification in the clinically relevant concentration range [10]. When ARChip Epoxy is used for colorimetric detection the linear range covers 0.1 ng/mL to 10 ng/mL S-100 which is one order of magnitude less than with colorimetric detection on nitrocellulose slides. The cut-off value lies within the linear range which means that normal levels can be well distinguished from pathologically elevated levels but quantification of higher serum levels is due to the narrow range difficult.

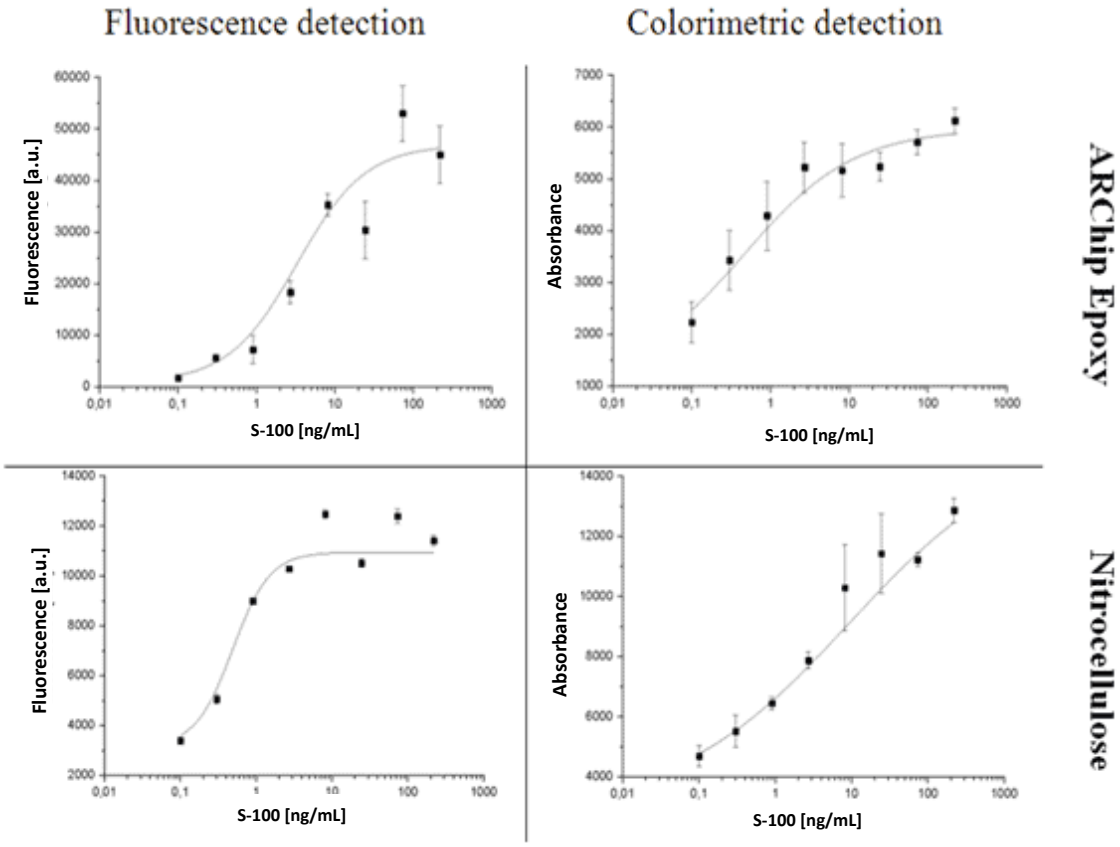

Figure 40: Calibration curves for S-100 using fluorescence and colorimetric detection on ARChip Epoxy and nitrocellulose slides.

Table 3 shows the calculated limits of detection and mean coefficients of variation for fluorescence and colorimetric detection on either ARChip Epoxy or nitrocellulose. For all analytes tested, the CV decreases by 3 to 20 % in colorimetric detection with alkaline phosphatase: Coefficients of variation do not exceed 12 % in colorimetric assay but are ranging from about 14 to 31 % in fluorescence detection. While the limits of detection are the same for S-100 in both detection methods, the LOD's for IL-8 and CRP are even improved with colorimetric detection which corresponds well to the results of Petersen et al. (2007) who discovered similar or better sensitivity in AP detection of mutations of the ß-globin gene compared to fluorescence detection [24].

These results clearly indicate that the detection with alkaline phosphatase on nitrocellulose slides can replace fluorescence detection without compromise in assay sensitivity. In addition, larger linear ranges (up to 1000-fold) are obtained, which improved data reproducibility (CVs are reduced by 3 to 20 %) at comparable limits of detection.

Table 3: LODs and mean CVs in % of fluorescence detection of S-100, IL-8 and CRP using nitrocellulose and ARChip Epoxy slides.

Analyte	strp-Dy647 on ARChip Epoxy	strp-AP on nitrocellulose
S-100 [ng/mL]	0.02 (13.9 %)	0.01 (11.0 %)
IL-8 [pg/mL]	6.70 (19.6 %)	1.34 (10.1 %)
CRP [µg/mL	- (30.8 %)	3.00 (11.7 %)

9 Conclusions

Microarray technology promises fast multiplexed screening of various biomarkers, only small sample volumes (< 40 µL) are needed for the sensitive detection of a biomarker panel. However, current costs of fluorescence-based microarray scanners are too high for wide use in diagnostic applications. Using colorimetric detection methods significant cost reductions can be achieved but are often associated with a loss in sensitivity and the need of well controlled assay conditions like temperature, development time and buffer composition.

We presented herein a protein microarray for the sensitive detection of IL-8, CRP and S-100 with colorimetric methods. Two colorimetric detection principles (enzymatic reaction and gold nanoparticles combined with silver staining) were evaluated for the detection of S-100. Several assay parameters such as the assay buffer, streptavidin concentration and the chip substrate were optimized. The colorimetric method performing best in terms of sensitivity, reproducibility and assay time was used for the simultaneous detection of the biomarker panel, consisting of three biomarkers of different size (IL-8: 8.4 kDa, CRP: 23 kDa, S-100: 9-13kDa) and different cut-off value (IL-8: 20 pg/mL, CRP: 10 µg/mL, S-100: 10 ng/mL). To establish the on-chip assays, two different assay architectures (sandwich assay, binding inhibition assay) were implemented. The biomarkers were detected at clinically relevant concentrations and compared to the conventional, fluorescence-based approach. For colorimetric detection a digital camera (about 500 EUR) was used instead of a costly microarray scanner (about 60.000 EUR).

Nitrocellulose showed highest signal intensities using colorimetric detection, lowest LOD was achieved with alkaline phosphatase and BCIP/NBT as enzyme substrate. Colorimetric detection with nitrocellulose as chip substrate leaded to comparable or even better limits of detection compared to the conventional fluorescence-based approach, the reproducibility defined by the CV in % was improved by 4 to 20 %. Both colorimetric and fluorescence detection were particularly appropriate for detecting elevated levels of S-100. For the detection of CRP more sensitivity is needed, while the on-chip assay for IL-8 allows sensitive and reliable classification of the disease. The assay handling in colorimetric detection was similar to that in fluorescence detection while the drawbacks of needing sophisticated scanning devices and the effect of fluorescence quenching and photobleaching are avoided. On the other hand colorimetric detection requires well controlled assay conditions to obtain reliable analysis data. Especially color development time makes standardized or even automated read-out difficult.

Though some technical hurdles still need to be overcome the results illustrate that the colorimetric approach can replace fluorescence detection without loss in sensitivity or reproducibility but being more cost-effective. Different biomarkers in different concentration ranges, of different sizes and in different assay architectures could be detected sensitively; which indicates that this approach can be adapted to various biomarker panels and concentration ranges.

10 Bibliography

[1] W. Wei, C. Zhang, J. Qian, and S. Liu, “Multianalyte immunoassay chip for detection of tumor markers by chemiluminescent and colorimetric methods.,” *Analytical and Bioanalytical Chemistry*, pp. 3269–3274, Sep. 2011.

[2] R. P. Ekins, “Ligand assays: from electrophoresis to miniaturized microarrays.,” *Clinical Chemistry*, vol. 44, no. 9, pp. 2015–30, Sep. 1998.

[3] H.-J. Müller and T. Röder, *Der Experimentator: Microarrays*, 1st ed. München: Elsevier GmbH, Spektrum Akademischer Verlag, 2004.

[4] L. Sage, “Biochips Go High-Tech,” *Analytical Chemistry*, vol. 76, no. 7, p. 137A–42A, 2004.

[5] U. Sauer, P. Domnanich, and C. Preininger, “Protein chip for the parallel quantification of high and low abundant biomarkers for sepsis.,” *Analytical Biochemistry*, vol. 419, no. 1, pp. 46–52, Dec. 2011.

[6] K. V. Lemley, “An introduction to biomarkers: applications to chronic kidney disease.,” *Pediatric Nephrology (Berlin, Germany)*, vol. 22, no. 11, pp. 1849–59, Nov. 2007.

[7] I. Biomarkers Definitions Working Group, “Biomarkers and surrogate endpoints: preferred definitions and conceptual framework,” *Clinical Pharmacology and Therapeutics*, vol. 69, no. 3, pp. 89–95, 2001.

[8] E. Society, “White paper on imaging biomarkers.,” *Insights into Imaging*, vol. 1, no. 2, pp. 42–45, May 2010.

[9] J. a Martius, T. Roos, B. Gora, M. K. Oehler, L. Schrod, T. Papadopoulos, and U. Gross, “Risk factors associated with early-onset sepsis in premature infants.,” *European Journal of Obstetrics, Gynecology, and Reproductive Biology*, vol. 85, no. 2, pp. 151–8, Aug. 1999.

[10] P. Buchegger, U. Sauer, H. Toth-Székély, and C. Preininger, “Miniaturized protein microarray with internal calibration as point-of-care device for diagnosis of neonatal sepsis,” *Sensors*, vol. 12, pp. 1494–1508, 2012.

[11] M. Baggiolini and I. Clark-Lewis, “IL-8, a chemotactic and inflammatory,” *Federation of European Biochemical Societies*, vol. 307, no. I, pp. 97–101, 1992.

[12] C. Pierrakos and J.-L. Vincent, “Sepsis biomarkers: a review,” *Critical Care*, vol. 14, no. 1, p. R15, 2010.

[13] G. R. Stryjewski, E. S. Nylen, M. J. Bell, R. H. Snider, K. L. Becker, A. Wu, C. Lawlor, and H. Dalton, “Interleukin-6, interleukin-8, and a rapid and sensitive assay for calcitonin precursors for the determination of bacterial sepsis in febrile neutropenic children.,” *Pediatric Critical Care Medicine a Journal of the Society*

of Critical Care Medicine and the World Federation of Pediatric Intensive and Critical Care Societies, vol. 6, no. 2, pp. 129–135, 2005.

[14] O. Livaditi, A. Kotanidou, A. Psarra, I. Dimopoulou, C. Sotiropoulou, K. Augustatou, C. Papasteriades, A. Armaganidis, C. Roussos, S. E. Orfanos, and E. E. Douzinas, "Neutrophil CD64 expression and serum IL-8: sensitive early markers of severity and outcome in sepsis.," *Cytokine*, vol. 36, no. 5–6, pp. 283–90, Dec. 2006.

[15] H. Ablij and A. Meinders, "C-reactive protein: history and revival.," *European Journal of Internal Medicine*, vol. 13, no. 7, p. 412, Oct. 2002.

[16] J. P. Tappero E., "Laboratory evaluation of neonatal sepsis," *Newborn and Infant Nursing Reviews*, vol. 10, pp. 209–217, 2010.

[17] R. Wolf, T. Ruzicka, and S. H. Yuspa, "Novel S100A7 (psoriasin)/S100A15 (koebnerisin) subfamily: highly homologous but distinct in regulation and function.," *Amino Acids*, vol. 41, no. 4, pp. 789–96, Oct. 2011.

[18] A. A. Hsu, K. Fenton, S. Weinstein, J. Carpenter, H. Dalton, and M. J. Bell, "Neurological injury markers in children with septic shock.," *Pediatric Critical Care Medicine a Journal of the Society of Critical Care Medicine and the World Federation of Pediatric Intensive and Critical Care Societies*, vol. 9, no. 3, pp. 245–251, 2008.

[19] M. Helm and S. Wölfl, *Instrumentelle Bioanalytik*, 1st ed. Heidelberg: WILEY-VCH Verlag GmbH & Co. KGaA, Weinheim, 2007.

[20] G. C. Le Goff, B. P. Corgier, C. a Mandon, G. De Crozals, C. Chaix, L. J. Blum, and C. a Marquette, "Impact of immobilization support on colorimetric microarrays performances.," *Biosensors & Bioelectronics*, vol. 35, no. 1, pp. 94–100, May 2012.

[21] R.-Q. Liang, C.-Y. Tan, and K.-C. Ruan, "Colorimetric detection of protein microarrays based on nanogold probe coupled with silver enhancement.," *Journal of Immunological Methods*, vol. 285, no. 2, pp. 157–63, Feb. 2004.

[22] L. Jiang, Z. Yu, W. Du, Z. Tang, T. Jiang, C. Zhang, and Z. Lu, "Development of a fluorescent and colorimetric detection methods-based protein microarray for serodiagnosis of TORCH infections.," *Biosensors & Bioelectronics*, vol. 24, no. 3, pp. 376–82, Nov. 2008.

[23] J. Tang, L. Zhou, L. L. Duan, Y. Feng, X. Cao, and Y. Wang, "Development and evaluation of a new detection tool-visual DNA microarray for simultaneous and specific detection of human immunodeficiency virus type-1 and hepatitis C virus.," *Molecular Biology Reports*, Feb. 2011.

[24] J. Petersen, M. Stangegaard, H. Birgens, and M. Dufva, "Detection of mutations in the beta-globin gene by colorimetric staining of DNA microarrays visualized by a flatbed scanner.," *Analytical Biochemistry*, vol. 360, no. 1, pp. 169–71, Jan. 2007.

[25] M. Cretich, V. Sedini, F. Damin, M. Pelliccia, L. Sola, and M. Chiari, “Coating of nitrocellulose for colorimetric DNA microarrays.,” *Analytical Biochemistry*, vol. 397, no. 1, pp. 84–8, Feb. 2010.

[26] F. Lottspeich and J. Engels, *Bioanalytik*, 2nd ed. Spektrum Akademischer Verlag Heidelberg 2009, Springer, 2009, pp. 1–1119.

[27] R. P. Ekins and F. W. Chu, “Multianalyte microspot immunoassay. The microanalytical ‘compact disk’ of the future,” *Clinical Chemistry*, vol. 37, no. 11, pp. 1955–1967, 1991.

[28] U. R. Müller and D. V. Nicolau, *Microarray Technology and Its Applications*. Springer-Verlag Berlin Heidelberg, 2005.

[29] C. Preininger and U. Sauer, “Quality control of chip manufacture and chip analysis using epoxy-chips as a model,” *Sensors and Actuators B: Chemical*, vol. 90, no. 1–3, pp. 98–103, Apr. 2003.

[30] P. Soundy and B. Harvey, “Western Blotting as a Diagnostic Method,” in *Medical Biomethods Handbook*, J. M. Walker and R. Rapley, Eds. Humana Press, 2005, pp. 43–62.

[31] K. Geckeler, *Bioanalytische und biochemische Labormethoden*. Vieweg & Sohn Verlagsgesellschaft m. b. H., 1998.

[32] M. Schena, R. A. Heller, T. P. Theriault, K. Konrad, E. Lachenmeier, and R. W. Davis, “platform for functional genomics,” *Tibtech*, vol. 16, no. July, pp. 301–306, 1998.

[33] W. Zhang, C.-Y. Xue, and K.-L. Yang, “A method of printing uniform protein lines by using flat PDMS stamps.,” *Journal of Colloid and Interface Science*, vol. 353, no. 1, pp. 143–8, Jan. 2011.

[34] T. Das, S. K. Mallick, D. Paul, S. K. Bhutia, T. K. Bhattacharyya, and T. K. Maiti, “Microcontact printing of Concanavalin A and its effect on mammalian cell morphology.,” *Journal of Colloid and Interface Science*, vol. 314, no. 1, pp. 71–9, Oct. 2007.

[35] B. B. Haab, M. J. Dunham, and P. O. Brown, “Protein microarrays for highly parallel detection and quantitation of specific proteins and antibodies in complex solutions,” *Genome Biology*, vol. 2, no. 2, pp. 1–22, 2000.

[36] M. Gonzalez-Gonzalez, R. Jara-Acevedo, S. Matarraz, M. Jara-Acevedo, S. Paradinas, J. M. Sayagües, A. Orfao, and M. Fuentes, “Nanotechniques in proteomics: Protein microarrays and novel detection platforms.,” *European Journal of Pharmaceutical Sciences : Official Journal of the European Federation for Pharmaceutical Sciences*, Jul. 2011.

[37] J. T. Andersson, M. Faust, J. Bettmer, H. Freitag, W. Buscher, O. Geschke, A. Cammann, Karl, Höner, U. Chemnitus, Gabriele-Christine, Karst, C. Dumschat, and A. Katerkamp, *Instrumentelle Analytische Chemie*. 2001.

[38] S. Basuray, L. Capretto, H.-C. Chang, H.-W. Chen, L.-J. Cheng, W. Cheng, T. D. Chung, H. Gai, X. Gong, M. Hill, K. Kawai, H. X. Kim, Y. Li, B. Lin, X. Liu, S. K. Njoroge, J. Noh, D. Noort, J. K. Osiri, J. Qin, S. Senapati, H. Shadour, S. Shi, W., Shoji, Z. Slouka, S. A. Soper, L. Wang, H. Wen, W. Wen, M. A. Witek, H. Xie, E. S. Yeung, S. Zeng, C. Zhang, and X. Zhang, *Microfluidics: Technologies and Applications*. Springer-Verlag Berlin Heidelberg, 2011, pp. 1–339.

[39] S. Nagl, M. Schaeferling, and O. S. Wolfbeis, "Fluorescence Analysis in Microarray Technology," *Microchimica Acta*, vol. 151, no. 1–2, pp. 1–21, Aug. 2005.

[40] Dyomics GmbH, "DY-630." [Online]. Available: http://www.dyomics.com/red-excitation.html. [Accessed: 25-Aug-2012].

[41] H. Päkkilä and T. Soukka, "Simple and inexpensive immunoassay-based diagnostic tests," *Bioanalytical Reviews*, vol. 3, no. 1, pp. 27–40, Feb. 2011.

[42] M. H. Gey, *Instrumentelle Analytik und Bioanalytik*, 2nd ed., no. Ic. Springer-Verlag Berlin Heidelberg, 2008.

[43] C. Hempen and U. Karst, "Labeling strategies for bioassays.," *Analytical and Bioanalytical Chemistry*, vol. 384, no. 3, pp. 572–83, Feb. 2006.

[44] I. Bio-Rad Laboratories, "Protein Blotting Guide: A Guide to Transfer and Detection," 3rd ed., Bio-Rad Laboratories, Inc., 2010, pp. 1–78.

[45] I. Alexandre, S. Hamels, S. Dufour, J. Collet, N. Zammatteo, F. De Longueville, J. L. Gala, and J. Remacle, "Colorimetric silver detection of DNA microarrays.," *Analytical Biochemistry*, vol. 295, no. 1, pp. 1–8, Aug. 2001.

[46] P. Domnanich, U. Sauer, J. Pultar, and C. Preininger, "Protein microarray for the analysis of human melanoma biomarkers," *Sensors and Actuators B: Chemical*, vol. 139, no. 1, pp. 2–8, May 2009.

[47] U. Sauer, J. Pultar, and C. Preininger, "Critical role of the sample matrix in a point-of-care protein chip for sepsis.," *Journal of Imunological Methods*, vol. 378, no. 1–2, pp. 44–50, Apr. 2012.

[48] Z. Ma and S.-F. Sui, "Naked-Eye Sensitive Detection of Immunoglubulin G by Enlargement of Au Nanoparticles in Vitro," *Angewandte Chemie (Int. ed. in english)*, vol. 41, no. 12, pp. 2176–2179, 2002.

[49] H. Rehm and T. Letzel, *Der Experimentator: Proteinbiochemie/Proteomics*, 6th ed. Heidelberg: Spektrum Akademischer Verlag Heidelberg 2010, Springer, 2010.

[50] M. Schena, *Microarray Analysis*. New York: Wiley-Liss, 2003.

[51] M. Walther, B. Stillman, A. Friße, and J. Beator, "The FAST Guide to Protein Microarrays." Whatman Schleicher & Schuell, pp. 1–27.

[52] B. Batteiger, W. J. Newhall, and R. B. Jones, “The use of Tween 20 as a blocking agent in the immunological detection of proteins transferred to nitrocellulose membranes,” *Journal of Immunological Methods*, vol. 55, no. 3, pp. 297–307, 1982.

[53] F. Ausubel, M. Brent, R. Kingston, D. D. Moore, J. G. Seidman, J. A. Smith, and K. Struhl, *Current protocols in Molecular Biology*. New York: Greene and Wiley-Interscience, 1987.

[54] R. Graf and P. Friedl, “Detection of immobilized proteins on nitrocellulose membranes using a biotinylation-dependent system.,” *Analytical Biochemistry*, vol. 273, no. 2, pp. 291–7, Sep. 1999.

[55] C. Yu, M. Liu, I. Kuan, and S. Lee, “Low-Density Protein Microarray on Nitrocellulose Membrane for the Detection of Human Cytokines,” *Cytokine*, vol. 18, no. 1, pp. 15–22, 2006.

[56] V. Espina, E. C. Woodhouse, J. Wulfkuhle, H. D. Asmussen, E. F. Petricoin, and L. a Liotta, “Protein microarray detection strategies: focus on direct detection technologies.,” *Journal of Immunological Methods*, vol. 290, no. 1–2, pp. 121–33, Jul. 2004.

[57] C. P. Paweletz, L. Charboneau, V. E. Bichsel, N. L. Simone, T. Chen, J. W. Gillespie, M. R. Emmert-Buck, M. J. Roth, E. F. Petricoin III, and L. a Liotta, “Reverse phase protein microarrays which capture disease progression show activation of pro-survival pathways at the cancer invasion front.,” *Oncogene*, vol. 20, no. 16, pp. 1981–9, Apr. 2001.

[58] “SPI-Mark Colloidal Gold Reagents - Immunogold Labeling - SPI Supplies.” [Online]. Available: http://www.2spi.com/catalog/chem/immunogold_labelling.php. [Accessed: 13-Aug-2012].

[59] M. Bendayan, “Colloidal Gold Post-Embedding Immunocytochemistry,” *Progress in Histochemistry and Cytochemistry*, vol. 29, no. 4, p. III–159, Jan. 1995.

[60] N. Tippkötter, H. Stückmann, S. Kroll, G. Winkelmann, U. Noack, T. Scheper, and R. Ulber, “A semi-quantitative dipstick assay for microcystin.,” *Analytical and bioanalytical chemistry*, vol. 394, no. 3, pp. 863–9, Jun. 2009.

[61] D. H. Choi, S. K. Lee, Y. K. Oh, B. W. Bae, S. D. Lee, S. Kim, Y.-B. Shin, and M.-G. Kim, “A dual gold nanoparticle conjugate-based lateral flow assay (LFA) method for the analysis of troponin I.,” *Biosensors & Bioelectronics*, vol. 25, no. 8, pp. 1999–2002, Apr. 2010.

[62] C. Albrecht, P. Fechner, D. Honcharenko, L. Baltzer, and G. Gauglitz, “A new assay design for clinical diagnostics based on alternative recognition elements.,” *Biosensors & bioelectronics*, vol. 25, no. 10, pp. 2302–8, Jun. 2010.

11 Index of Figures

12 Poster Europtrode Barcelona 2012

AUSTRIAN INSTITUTE OF TECHNOLOGY

Development of a colorimetric sepsis tube array using a digital camera for read-out

H. Herzog, P. Buchegger, C. Preininger
AIT Austrian Institute of Technology, Health & Environment Department, Bioresources, Konrad Lorenz Straße 24, 3430 Tulln, Austria

heidelinde.herzog@ait.ac.at

Integration of lasers as light source and photomultipliers for detection make scanning equipment for fluorescence-based chip analysis sophisticated and expensive. Health authorities are faced with limited resources; hence, simple, robust and inexpensive methods and instrumentation providing the same quality and sensitivity are urgently needed.
In order to meet this demand, a multianalyte immunoassay for simple, portable and low-cost quantification of C-reactive protein (CRP), Interleukin-8 (IL-8) and S-100 based on colorimetric detection using a digital camera for read-out was developed. 8-well strips, transparent and non-transparent surfaces were compared to find the most suitable spotting substrate for colorimetric detection.
Results demonstrate that assay sensitivity is similar to that of the fluorescence-based chip, showing that the colorimetric assays can replace fluorescence based devices without compromise in sensitivity but being more cost-effective.

Principle of the colorimetric assays

Fig. 1: Scheme of sandwich immunoassays with enzyme detection (left) and gold label silver staining (right)

Three colorimetric methods based on enzymatic detection with either alkaline phosphatase ("AP") or horse radish peroxidase polymer ("HRPp") and detection with gold nanoparticles ("AuNP") and subsequent silver staining were evaluated using BSA/antigen conjugates [1] as spotted probes. Detection and quantification was performed by immunoreactions with biotinylated detection antibodies and streptavidin labeled with either gold nanoparticles, AP or HRPp. The bound nanoparticles were enlarged with $HAuCl_4$ and NH_2OH * HCl [2] and visualized through silver staining. Enzymatic reactions were fulfilled with either Diaminobenzidine (HRP) or BCIP/NBT (AP) as substrate. Subsequent colorimetric detection was done with either ClonDiag ArrayMate or a digital camera (Nikon 3000D).

Evaluation of colorimetric detection methods

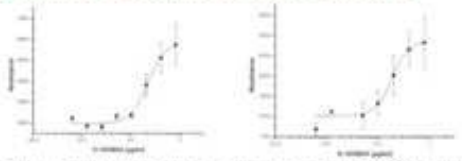

Fig. 2: Semilogarithmic standard curves for spotted S-100/BSA conjugates and detection with alkaline phosphatase (left) and horse radish peroxidase polymer (right).

Fig. 3: Images of S-100/BSA detected with: a) AuNP b) AuNP and gold precipitation c) AuNP and silver staining, d) AuNP, gold precipitation and silver staining

Detection with AP labeled streptavidin shows higher signal intensities and lower coefficients of variation than detection with HRPp. Signals were observed with silver stained Au nanoparticles; additional gold precipitation before silver staining results in even higher signal intensities and lower coefficents of variation.

Colorimetric vs. fluorescence detection

	Fluorescence		AP	
Analyte	NC	ARC	NC	ARC
S-100 [pg/well]	0.94 (1.8%)	0.82 (13.9%)	0.01 (11.8%)	2.64 (16.4%)
IL-8 [pg/well]	18.37 (2.8%)	6.70 (19.6%)	1.34 (10.1%)	0.01 (4.8%)
CRP [ng/well]	1.64 (3.4%)	- (36.8%)	3.00 (11.7%)	- (7.4%)

Table 1:LODs and mean CVs (in %) using fluorescence and AP detection on nitrocellulose ("nc") and ARChip Epoxy ("ARC") for sandwich assays of S-100, IL-8 and binding inhibition assay of CRP

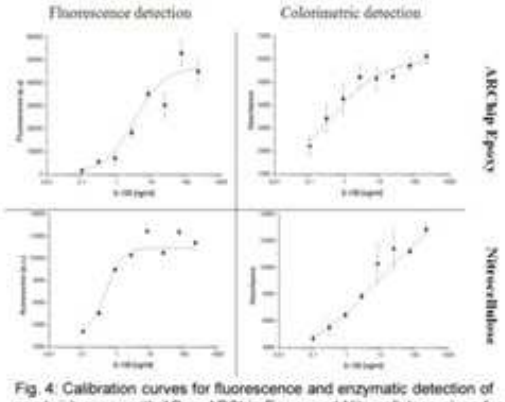

Fig. 4: Calibration curves for fluorescence and enzymatic detection of sandwich assay with AP on ARChip Epoxy and Nitrocellulose given for S-100 as an example

Conclusion:
Among the tested detection methods, AP shows lowest LODs and coefficients of variation. Nitrocellulose slides showed the biggest dynamic ranges for colorimetric detection of S-100, IL-8 and CRP. The thoughtful choice of suitable spotting substrates for sensitive and reproducible colorimetric detection is crucial.

REFERENCES
[1] Buchegger, P.; Sauer, U.; Toth-Székély, H.; Preininger, C. Miniaturized Protein Microarray with Internal Calibration as Point-of-Care Device for Diagnosis of Neonatal Sepsis. Sensors 2012, 12, 1494-1508.
[2] Ma, Z.F.; Sui, S.F. Naked-Eye Sensitive Detection of Immunoglubulin G by Enlargement of Au Nanoparticles In Vitro. Angew. Chem. Int. Ed. 2002, 41, 2176-2179.